Håvard Gullik Sørbø

Characterization of the C-type lectin receptor Mincle in *Mycobacterium avium*-infected macrophages

Master's thesis in Molecular medicine

Trondheim, June 2016

Principal supervisor: Trude Helen Flo

Co-supervisors: Signe Elisabeth Åsberg and Jenny Ostrop

Norwegian University of Science and Technology (NTNU)
Faculty of medicine
Department of Cancer Research and Molecular Medicine,
Centre of Molecular Inflammation Research (CEMIR)

NTNU
Norwegian University of Science and Technology

CEMIR
Centre of Molecular Inflammation Research

Abstract

Non-tuberculous diseases caused by opportunistic pathogens such as *Mycobacterium avium* are becoming more prevalent and has surpassed tuberculosis in developed countries. Trehalose-6,6-dimycolate (TDM) is recognized by the C-type lectin receptor Mincle, it is an abundant glycolipid in the cell wall of mycobacteria and a major virulence factor. Yet, the role of Mincle in mycobacterial infection models has been reported controversially. It varies between mycobacterial species, and the role of Mincle in *M. avium* infection has not yet been assessed. Using a murine *in vitro* model, we found that wild type and Mincle-deficient bone marrow-derived macrophages (BMMs) did not differ in their capability to phagocytose or kill *M. avium*, and no differences were observed for secreted amounts of KC, IL-6, IP-10 or G-CSF.

The localization of Mincle and its trafficking during mycobacterial infection is still not fully elucidated. In order to being able to study the localization of Mincle during *M. avium* infection, we tested and established tools. FcRγ is essential for Mincle signalling and suggested to be required for surface localization of Mincle. In this study, FcRγ was found to be beneficial, but not essential for surface expression of Mincle in transiently transfected HEK293 cells, in line with previous research. Mincle-specific antibodies were identified by flow cytometry and its application confirmed also for confocal microscopy. Although antibodies were found to be specific in overexpressing HEK293 cells, some background was observed in Mincle$^{-/-}$ BMMs. Overexpression of tagged- and untagged Mincle in primary BMMs and bone marrow-derived dendritic cells was achieved by retroviral transduction. In HEK293 cells transiently transfected with Mincle + FcRγ, Mincle was localized to the plasma membrane and around the nucleus, while preliminary results from transduced primary BMM/DCs indicated a more outspread localization of Mincle. Preliminary results from transduced BMMs infected with *M. avium* did not indicate an increased concentration of Mincle around the phagocytosed mycobacteria.

In summary, Mincle was not implicated to have an essential role in *M. avium* infection (≤ 5 d). While preliminary results indicated an outspread localization of Mincle in primary BMM/DCs, the tools established in this study can be used in future experiments to further elucidate the role Mincle upon mycobacterial infections.

Blank

Acknowledgements

This master project was carried out from August 2015 – June 2016, at the Centre of Molecular Inflammation Research (CEMIR), Department of Cancer Research and Molecular Medicine (IKM), NTNU.

First of all, I would like to express my gratitude to my supervisors, professor Trude Helen Flo, Signe Elisabeth Åsberg and Dr. Jenny Ostrop. Trude, thanks for trusting me and letting me take part in this project, even though my official status as a master student was not confirmed until several months later. Signe, you have taught me how to behave in a lab, proper sterile techniques and a bunch of methods, and I think you shaped me well. You introduced me to how science is conducted in real life, and your enthusiasm for science is contagious. Thanks for always being available and answering my questions, also outside of office-hours, especially the last weeks of my work. Jenny, your knowledge about C-type lectin receptors is admirable, you can safely entitle yourself as a CLR-guru. You have also taught me a whole lot of methods, and tips and tricks in the lab. Although it sometimes felt like you overestimated me, I am really grateful that you helped me plan and conduct experiments even though I did not always see the light in the end of the tunnel. Thanks for answering questions and giving me feedback on my writing over and over again, you are possibly the most efficient person I know of.

Experiments conducted would not have been possible without the generous gift of Mincle$^{-/-}$ cells from Christine Wells. I would also like to thank Anne Marstad and Claire Louet for help with qPCR measurements and data analysis, and Kjartan Egeberg, Bjørnar Sporsheim and Alexandre Gidon for teaching me confocal imaging and helping me along the way. To the rest of the Mycobacteria Group: thanks for answering all my questions in and outside the lab, showing me how things work and laughing of my jokes (Hany Ibrahim, Marianne S. Beckwith).

Lastly, I would like to thank my family and friends for their support and patience. Thank you Arne Lindefjeld and Kjell Sjøberg for proof-reading, and thank you Katarina Utne, for continuous encouragement and lighting up my days the whole year through.

Håvard Gullik Sørbø, Trondheim, June 2016

Blank

Contents

Abbreviations

BCG	Bacille Calmette-Guerin
BM	Bone marrow
BMDC	Bone marrow-derived dendritic cell
BMM	Bone marrow-derived macrophage
CARD	Caspase recruitment domain-containing protein
CFP	Cyan fluorescent protein
CLR	C-type Lectin receptor
DAMP	Danger/damage-associated molecular pattern
ELISA	Enzyme-linked immunosorbent assay
FcRγ	Fc-ε-receptor I gamma (γ)
G-CSF	Granulocyte-colony stimulating factor
GFP	Green fluorescent protein
HA	Hemagglutinin
HIV	Human immunodeficiency virus
IFN-γ	Interferon gamma (γ)
IL	Interleukin
IP-10	Interferon gamma-induced protein (also, CXCL10)
ITAM	Immunoreceptor tyrosine-based activation motif
ITIM	Immunoreceptor tyrosine-based inhibitory motif
KC	Keratinocyte-derived protein chemokine (murine homolog of IL-8)
LPS	Lipopolysaccharide
MAC	*Mycobacterium avium-intracellulare* complex
Mcl	Macrophage C-type lectin
MDR	Multi-drug resistant
Mincle	Macrophage-inducible C-tyle lectin
MOI	Multiplicity of infection
Mtb	*Mycobacterium tuberculosis*
MTC	*Mycobacterium tuberculosis* complex
NF-κB	Nuclear factor kappa-light-chain-enhancer of activated B cells
NLR	Nod-like receptor
NTM	Non-tuberculous mycobacteria
PAMP	Pathogen-associated molecular pattern
PRR	Pattern recognition receptor
RLR	RIG-I-like receptor
RNS	Reactive nitrogen species
ROS	Reactive oxygen species
Syk	Spleen tyrosine kinase
TB	Tuberculosis
TDB	trehalose-6,6'-dibehenate
TDM	trehalose-6,6'-dimycolate
TDR	Totally drug resistant
TLR	Toll-like receptor
WT	Wild type
XDR	Extensively drug resistant

1 Introduction

Mycobacterial infections constitute a considerable global health problem that give rise to extensive morbidity and causes a variety of diseases. The causing bacteria belong to the genus *Mycobacterium* which, as of today, includes around 180 named species (Parte, 2014). These species range from non-pathogenic environmental bacteria to obligate pathogens like *Mycobacterium tuberculosis* (Mtb), the causative agent for tuberculosis (TB). Mtb is, alongside human immunodeficiency virus (HIV), the leading cause of death by a single infectious agent. Mtb was responsible for approximately 1.5 million deaths in 2014, of which 0.4 million people were HIV-positive. An estimated one third of the world's population is thought to be latently or sub-clinically infected with Mtb, and 9.6 million people developed active TB in 2014 (WHO, 2015). Most cases were caused by the reactivation of dormant Mtb in latently infected hosts.

Since 1990, TB mortality has fallen by 47 % and an estimated 43 million lives have been saved between 2000 and 2014 due to improved diagnosis and treatment methods (WHO, 2015). Despite these major advances TB remains hard to treat, requiring long-term treatment with antibiotics. The emergence of multi-drug resistant (MDR), extensively (XDR) and totally resistant (TDR) Mtb are further complicating the issue of treatment (WHO, 2015). While TB is decreasing, there has been an increase in infection rates of non-tuberculous mycobacterial (NTM) diseases over the past few decades (Brode et al., 2014). Considering the extensiveness of Mtb, drug resistance and the reported incline in NTM diseases, a better understanding of mycobacteria, hosts and their interaction is needed to improve today's treatment of mycobacterial infections and make more effective vaccines.

1.1 Non-tuberculous mycobacteria: opportunistic neighbours

Apart from species included in the *Mycobacterium tuberculosis* complex (MTC), causing TB and TB-like diseases, the remaining majority of the bacteria in the genus *Mycobacterium* are considered NTM (Falkinham, 2009). These NTM range from obligate pathogens that barely replicate outside of a host (e.g. *M. leprae*), to true environmental mycobacteria (e.g. *M. avium*) that are opportunistic pathogens in humans, animals and birds (Kazda and Pavlik, 2009).

NTM are usually slow growing, but as oligotrophs, combined with their ability to form biofilms, they are good competitors in low nutrient environments (Falkinham, 2009; Schulze-Röbbecke et al., 1992). These characteristics have made mycobacteria inhabit a wide array of habitats;

various salt- and freshwater sources around the globe (Field et al., 2004), including drinking water pipelines (Thomson et al., 2013), shower heads (Falkinham III et al., 2008) and bottled water (Covert et al., 1999), coniferous forest soil (Iivanainen et al., 1997), house dust (Dawson, 1971) commercial potting soil (De Groote et al., 2006), and among sphagnum mosses, including on the west coast of Norway (Kazda and Pavlik, 2009), Canada (Cayer et al., 2007), and Madagascar (Schröder et al., 1992).

The findings span all continents and a range of various climates, but not all isolates were associated with human diseases. Worldwide, *Mycobacterium avium* complex (MAC) is the most common cause of NTM disease (Prevots and Marras, 2015). MAC includes several related species and subspecies, where the most commonly found are *M. avium*, *M. intracellulare*, *M. chimaera*, and *M. colombiense* plus subspecies (Ben Salah et al., 2008). Other common disease-causing NTM are *M. kansasii*, *M. ulcerans*, *M. abscessus*, *M. malmoense*, *M. marinum*, *M. xenopi* and *M. fortuitum* (Falkinham, 2009).

The incidence of NTM-associated diseases is increasing worldwide, also in developed countries (Brode et al., 2014), and reported rates of infections by NTM are thought to be underestimated (Prevots and Marras, 2015). NTM diseases are an important cause of disease in immunosuppressed individuals, but are becoming more common in post-menopausal women and older men with no recognized immune defects (Halstrom et al., 2015). The manifestations and risk factors of NTM infections are many. Generally, immunosuppressed individuals, elderly, and people with underlying diseases or a surgical history have a higher risk of acquiring an NTM disease (Cassidy et al., 2009). Disseminated disease or lymphadenitis is associated with more severe immune deficiencies, while infection in skin, bone or tissue can follow trauma at the affected site (Cassidy et al., 2009). In addition, pulmonary NTM infections are reported to affect otherwise healthy individuals (Halstrom et al., 2015). The manifestations of an NTM infection will vary between different NTM species, the type of exposure and the host's immune response. Around 50 % of all NTM infections are pulmonary, and the majority of these are caused by MAC (Henkle and Winthrop, 2015). The reported increase in diseases caused by various NTM are thought to be related to the HIV/AIDS epidemic, the widespread use of immunosuppressive therapy and an aging population (Cassidy et al., 2009), but also partly due to more sensitive laboratory diagnostic methods and increased awareness (Johnson and Odell, 2014).

1.2 Treatment of mycobacterial infections and vaccination status

Tuberculin skin tests (e.g. Mantoux, Pirquet) are used to examine if a person has previously been exposed to, and mounted an immune response against mycobacteria, but does not distinguish between Mtb/MTC and NTM (Hermansen et al., 2014). QuantiFERON-TB-gold-test is a test based on T-cell mediated IFN-γ release after stimulation with MTC-specific peptide antigens (Pottumarthy et al., 1999). Combined, the two tests can be used to discriminate between MTC and NTM. More precise determination can be achieved by a combination of radiography/high-resolution computer tomography (CT), and culturing of samples from sputum, biopsies or bronchial wash/lavage (van Ingen, 2013).

Mycobacterial infections are persistent and usually require combination therapy with 3–4 drugs given for 6–9 months or longer. Poor quality medicines, incorrect use of antimycobacterial drugs or premature termination of drug therapy can result in drug-resistant strains. For Mtb, XDR strains have been reported in 77 countries, and an estimated 50 million individuals carry MDR strains of Mtb, of which 480 000 people developed multidrug-resistant TB in 2014 (WHO, 2015). None of the drugs in use against NTM infections today were specifically developed for treating NTM diseases, most were developed for treating TB which might render them somewhat less effective (Egelund et al., 2015). Infections by NTM are thought to not always be correctly diagnosed (Prevots and Marras, 2015), which suggests that if patients are given antibiotics for only a brief period, medical doctors might actively and unknowingly select for drug-resistance among NTM.

The only licenced vaccine against Mtb in use today is Bacille Calmette-Guerin (BCG), a live vaccine based on attenuated strains of *M. bovis*. It has been used for nearly a century and is one of the most widely used vaccines. It has documented protective effects against disseminated TB and meningitis in children, but it does not prevent primary infection or reactivation of latent pulmonary infection in adults (WHO, 2015). The principal source of Mtb spread in the community is reactivation of latent pulmonary infection, and the impact by BCG vaccination on transmission of Mtb is therefore limited (WHO, 2015). The efficacy of the BCG vaccine also varies between geographical regions, which is suggested to be partly explained by a difference in exposure to various NTM species (Poyntz et al., 2014), and partly due to different BCG strains and cultivation procedures among different laboratories (Behr, 2002; Venkataswamy et al., 2012).

To reach WHOs goal of eliminating TB as a public health problem by 2050, a new vaccine against TB is needed (Kaufmann et al., 2015). There are currently 15 potential vaccines in clinical trials, of which eight are in phase II or IIb , and one is in phase III (Ahsan, 2015). These are divided into one recombinant BCG vaccine, one attenuated *M. tuberculosis* vaccine, three mycobacterial whole cell or extract vaccines, five protein/adjuvant vaccines and five viral vectored vaccines (Ahsan, 2015).

1.3 Mycobacterial characteristics

Mycobacteria are non-motile, aerobic and acid fast bacteria. Most species are slow-growing, and typically appear as straight or slightly curved rods; usually 3 – 5 µm long and 0.2 – 0.6 µm wide (Velayati and Farnia, 2012). Mycobacteria appear fuchsin-positive after Ziehl-Nelsen staining, but if treated with alkaline ethanol that remove the lipoid fraction, the mycobacteria lose their acid-fastness and becomes gram-positive (Murray et al., 1980). The thick, waxy and hydrophobic cell wall of mycobacteria is composed of a layer of glycolipids and a layer of peptidoglycan, held together by arabinogalactan, a polysaccharide (fig. 1.1).

1.3.1 Cord factor

The most abundant glycolipid in the cell wall of mycobacteria is trehalose-6,6'-dimycolate (TDM), also called cord factor (Zuber et al., 2008). TDM is a glycolipid consisting of a trehalose disaccharide attached to two long mycolic acids (C60 – C90) by an ester linkage (Noll et al., 1956). After its identification 60 years ago, TDM has been shown to be an important virulence factor that mediates resistance to host defences, reduces antigen presentation, delays phagosomal maturation and induces granuloma formation (Ryll et al., 2001). TDM has also been shown to be the most inflammatory-inducing component of the cell wall (Geisel et al., 2005). It causes adjuvanticity, contributes to cell recruitment and has shown anti-tumor activity, thereby having dual roles (Ryll et al., 2001).

That said, mycobacterial species differ in their composition of mycolic acids, and lipid extracts may contain a wide variety of different compounds, making it difficult to link any specific response to a particular (glyco-)lipid. Synthetic analogues can therefore be good alternatives to bacterial compounds, and trehalose-6,6'-dibehenate (TDB) is often used as an analogue to TDM.

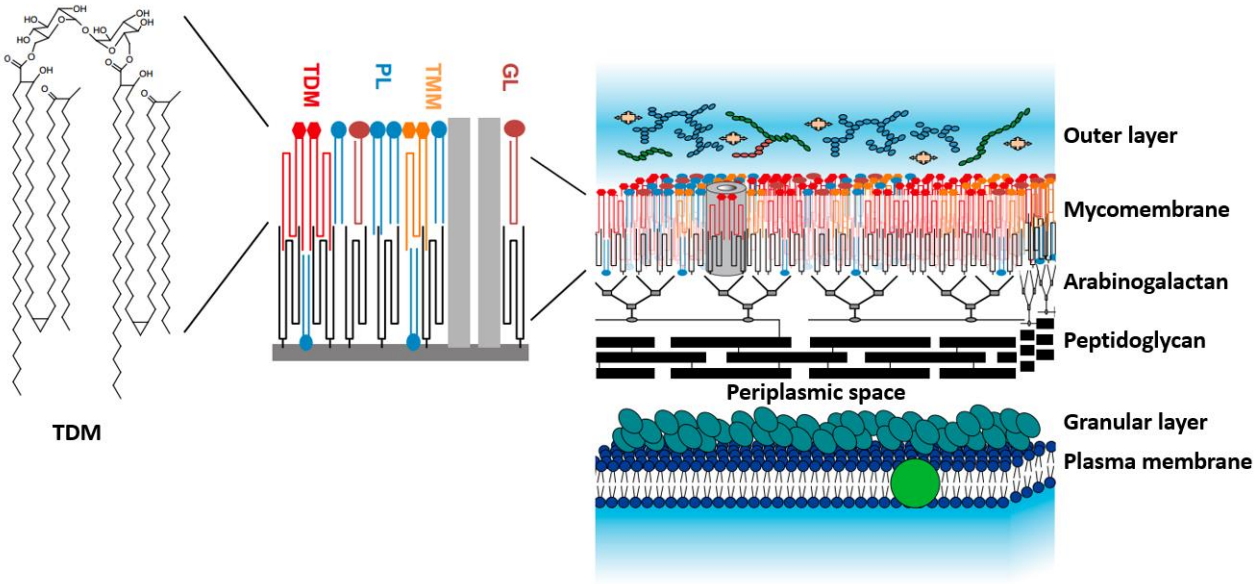

Figure 1.1 Simplified illustration of the mycobacterial cell wall. TDM: trehalose dimycolate, PL: phospholipids, TMM: trehalose monomycolate, GL: glycolipids. TDM with its long chains of mycolic acids is most likely folded to fit in a membrane of 7-8 nm and is here shown in a folded state. Molecules and layers are not drawn to scale. Adapted from (Marrakchi et al., 2014).

1.4 Immune responses to mycobacteria

After inhalation of aerosols containing infectious mycobacteria, bacilli are recognized by innate immune cells residing in the lungs, such as macrophages, neutrophils and dendritic cells (DC), which express a wide variety of receptors. Engagement of different pattern recognition receptors (PRRs) expressed by these innate immune cells induce the uptake of the pathogen through phagocytosis (Underhill and Goodridge, 2012). Macrophages combat microbial intruders by “eating” and digesting them, in a complex, but ordered process. Phagocytosis involves outreach- or invagination of the plasma membrane, ultimately leading to the formation of a phagosome (Aderem and Underhill, 1999). The pathogen-containing phagosome is now the organelle to which the host defence is targeted. Reactive nitrogen and oxygen species (RNS, ROS) is generated by the phagosomal enzymes inducible nitric oxide synthase (iNOS) and NAPDH phagocyte oxidase resulting in an oxidative burst. Acidification by proton pumps lowers the pH, which activates hydrolytic enzymes, and further damage of the pathogen is facilitated by antimicrobial peptides disturbing their cell membrane (Huynh and Grinstein, 2007). Phagolysosomal fusion is an essential step required for bacterial destruction and clearance (Gruenberg and Stenmark, 2004).

However, many mycobacterial species, including Mtb and *M. avium*, are able to inhibit phagosomal maturation and reside within infected macrophages (Ehrt and Schnappinger, 2009; Hestvik et al., 2005). This has been attributed to TDM, as mycobacteria increase TDM production after being phagocytosed (Fischer et al., 2001) and phagocytosed TDM-coated beads do not fuse with lysosomes (Indrigo et al., 2003). Infected macrophages that fail to eradicate the bacteria induce a local proinflammatory response which attracts other monocytes, and eventually this inflamed lesion matures into a granuloma; the hallmark of mycobacterial infection (Wagner and Young, 2004). Different types of granulomas can be distinguished, but often a granuloma is encircled by fibrous tissue that separates it from its surroundings. Within a granuloma mycobacteria can survive in an inactive/dormant state with very low but continuous respiration (Gengenbacher and Kaufmann, 2012), causing latent infection. Antimycobacterial drugs target functions essential for growth, which explains why they fail to eradicate nonreplicating mycobacteria (Zhang, 2004).

Mtb within granulomas can stay dormant for decades (Boon and Dick, 2012), with a constant risk of developing active infection. A state of dormancy has been observed in *M. avium*, which also cause granulomas (Archuleta et al., 2005). Reoccurring *M. avium*-infections have been observed over decades, both in immunosuppressed and immunocompetent individuals (Darouiche et al., 1996; Sridhar et al., 2016). The exact mechanisms of mycobacterial reactivation from latent infections are not known, but the risk of reactivation is increased whenever the immune system is compromised (Weiss and Schaible, 2015). Risk factors include HIV co-infection, diabetes, alcoholism, malnutrition and immuno-suppressive therapy (Flynn and Chan, 2001). Granulomas are usually formed in lung tissue, but disseminated disease or alternative routes of infection can lead to granuloma formation also in other organs. MAC is widespread in the environment, and swallowing of bacteria can lead to granuloma formation in liver and spleen, observed in both immunocompromised and immunocompetent patients (Farhi et al., 1986).

To control mycobacterial infections, different parts of the immune system need to interact, but the contribution of the different cell (sub-) types is yet not fully elucidated. Innate immune cells play a key role, and “trained immunity” by epigenetic alterations in innate cells in response to mycobacteria has been proposed to be of significance (Lerm and Netea, 2015). The importance of an adaptive response, especially by $CD4^+$ T helper cells that produce effector cytokines like interferon-γ (IFN-γ) and tumor necrosis factor alpha (TNF) is highlighted by the high incidence

of mycobacterial infections in patients with AIDS (Haug et al., 1996; WHO, 2015). IFN-γ secretion by T helper cells and subsequent macrophage activation is important for antimycobacterial defence mechanisms, as mutations in *IFNG* in humans are associated with higher susceptibility to mycobacterial infection (Dorman et al., 2004).

The role of $CD8^+$ T cells and B cells, as well as other subtypes (T_h17, T_{reg}, γδ T cells) upon mycobacterial infection is less known. Animal models have indicated a non-redundant role for $CD8^+$ T cells in Mtb infections, and humans generate specific classical (MHC I-restricted) and non-classical $CD8^+$ T cells in response to Mtb (Lin and Flynn, 2015). Autophagy has been shown to act as an immune effector, enhancing mycobacterial clearance (Gutierrez et al., 2004). Further, mycobacteria-specific T cells can restore autophagic flux in infected macrophages independent of IFN-γ (Petruccioli et al., 2012).

B cells are also activated during mycobacterial infections, and antibodies to Mtb are suggested to protect against disseminated spread of the bacilli (Costello et al., 1992). In addition, B cells can influence immune responses by modulating T cells, macrophages, DCs and neutrophils, although the importance of this contribution during mycobacterial infections remains unclear (Achkar et al., 2015).

1.4.1 Pattern recognition receptors

Different PRRs are expressed by innate immune cells, and several classes of PRRs are known. These germline-encoded sensors recognize conserved molecular patterns, both pathogen-associated molecular patterns (PAMPs) and danger/damage-associated molecular patterns (DAMPs).

Toll-like receptors (TLRs) are all membrane-bound, and together cover a broad ligand spectrum (Owen et al., 2013). TLR 1, 2, 4, 5 and 6 are located on the cell surface and recognize fungal, protozoal and bacterial PAMPs, for instance lipopolysaccharide (LPS) from gram-negative bacteria (TLR 4) and lipopeptides from gram-positive bacteria (TLR 1, 2 and 6). TLR 3, 7, 8 and 9 are exclusively expressed in endocytic compartments and recognize bacterial and viral nucleic acids, both RNA (TLR 3, 7, 8) and unmethylated CpG DNA (TLR 9). Activation of the different TLRs eventually leads to transcription of type I interferons, antimicrobial peptides and inflammatory cytokines.

Nucleotide-binding oligomerization domain receptors (NOD-like receptors; NLRs) and retinoic acid-inducible gene I protein helicase receptor (RIG-I-like receptors; RLRs) are exclusively cytoplasmic PRRs. There are three known RLRs; RIG-I, MDA5 and LGP2, all involved in antiviral responses, inducing inflammatory cytokines and type I interferons. NLRs sense diverse cytoplasmic PAMPs and DAMPs, and activation induces production and maturation of inflammatory cytokines.

Pathogens may express a wide variety of PAMPs recognized by different PRRs that together orchestrate an immune response. Several PRRs have been shown to sense mycobacteria, e.g. TLR 2 and TLR 4, the NRL NOD2 and different C-type lectin receptors (CLRs); Macrophage C-type lectin (Mcl), Dectin-1, Dendritic cell-specific intercellular adhesion molecule-3-grabbing non-integrin (DC-SIGN) and Macrophage inducible C-type lectin (Mincle) (Killick et al., 2013).

Mycobacterial infection studies using mice with single-PRR deletions show mild phenotypes (Mortaz et al., 2015). Deletion of caspase recruitment domain-containing protein 9 (CARD9), an essential downstream signalling protein of CLRs, leads to lethal outcomes of Mtb infections in mice (Dorhoi et al., 2010), highlighting the role of CLRs in mycobacterial infections.

1.4.2 C-type lectin receptors

CLRs comprise a large family of receptors divided into 17 groups based on functional and structural characteristics. CLRs contain calcium binding sites (hence, C-type) and one or more carbohydrate recognition domains (CRD). CLR ligands are diverse and include PAMPs and DAMPs. CLRs are traditionally associated with carbohydrate binding, although several CLRs can bind non-carbohydrate ligands. Many CLRs that are considered PRRs are transmembrane receptors localized in the natural killer (NK) gene cluster, and several belong in the Dectin-1 or Dectin-2 cluster (fig. 1.2). Notable exceptions are DC-SIGN and Mannose receptor C-type 1 (MRC1), that both have been shown to be involved in mycobacterial recognition (Killick et al., 2013).

Transmembrane CLRs can transduce intracellular signal via a motif within their cytoplasmic tail or be dependent on association with an adaptor molecule for signal transduction (fig. 1.3). Receptors in the Dectin-1 and Dectin-2 cluster signal through immunoreceptor tyrosine-based activation/inhibitory motifs (ITAMs/ITIMs). Receptors that are dependent on adaptor proteins

for signalling, e.g. Dectin-2, Mcl and Mincle signal through FcRγ, an ITAM-bearing adaptor protein, while other CLRs can signal through DAP12 (Dambuza and Brown, 2015). Upon binding and activation, tyrosine phosphorylation of the ITAM/ITAM-like motifs leads to recruitment and activation of Spleen tyrosine kinase (Syk). Further, activation of the CARD9-Bcl10-Malt1 scaffold through PKCδ result in translocation of the transcription factor Nuclear factor κB (NF-κB) and subsequent transcription of inflammatory cytokines (fig. 1.4) (Dambuza and Brown, 2015; Geijtenbeek and Gringhuis, 2009).

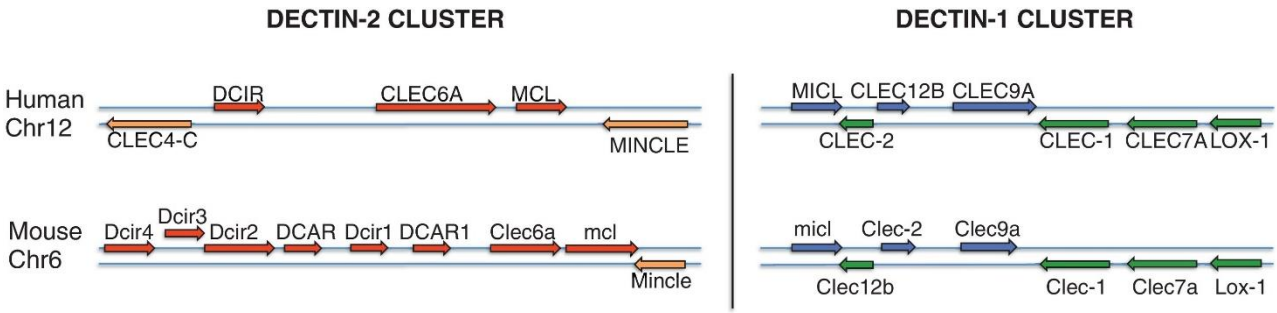

Figure 1.2 Genomic organization and orientation of CLRs in the Dectin-1 and Dectin-2 cluster. Both clusters are localized within the NK gene complex in humans and mice, on chromosome (Chr) 12 and 6, respectively. Obtained from (Dambuza and Brown, 2015)

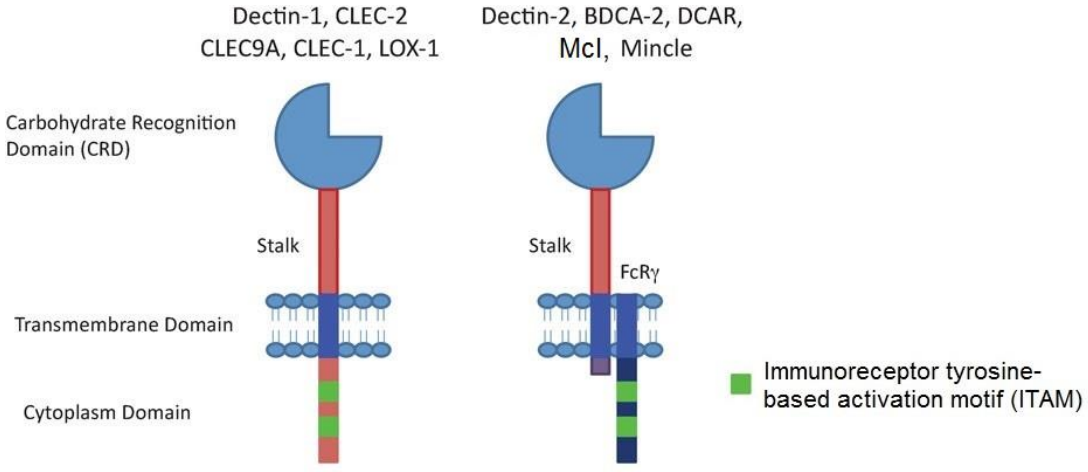

Figure 1.3 CLRs can signal through their cytoplasmic tail or via adaptor proteins, illustrated in this figure with members of Dectin-1 and Dectin-2 group. Often the cytoplasmic tail contains two ITAMs, but e.g. Dectin-1 has only one hemITAM. Adapted from (Kingeter and Lin, 2012).

1.4.3 Mincle

TDM has long been known to be an important virulence factor, to be an abundant glycolipid of the mycobacterial cell wall, and TDM alone induce granuloma formation (Bekierkunst et al., 1969). Yet, its receptor was not known before 2009, when Ishikawa et al. showed direct recognition of TDM by Mincle (Ishikawa et al., 2009). They also showed that Mincle-deficient mice do not induce granulomas from TDM alone, in contrast to wild type (WT). Mincle is expressed by immune cells including macrophages, DCs, neutrophils and some subsets of B cells (Kawata et al., 2012). Mincle has been shown to have a diverse ligand spectrum, including various glycolipids (Ishikawa et al., 2013), the nucleo-protein SAP130 (Yamasaki et al., 2008), cholesterol crystals (Kiyotake et al., 2015) and, atypically for CLRs, no carbohydrates so far (Graham et al., 2012).

Mincle has a short cytosolic N-terminal tail and depend on the ITAM-bearing adaptor protein FcRγ for signalling (Yamasaki et al., 2008). Downstream signalling (fig. 1.4) leads to transcription of inflammatory cytokines, e.g. TNF, IL-8/KC/MIP-2 and IL-6, but also anti-inflammatory IL-10 (Kerscher et al., 2013). Together, the cytokines and chemokines contribute to shape naïve T cells into effector T helper (T_H1, T_H17) subtypes (Smith and Williams, 2016). Mincle and Mcl share sequence similarities, and although the adaptor protein for Mcl is unclear, Mcl signal through Syk (Graham et al., 2012). Heterodimerization of murine Mincle/Mcl (Lobato-Pascual et al., 2013; Miyake et al., 2015) and Mcl/Dectin-2 (Zhu et al., 2013) have been suggested based on co-precipitation. However, a functional difference between human and murine Mincle and Mcl has been implicated, as human Mincle and Mcl was not co-precipitated, contrary to murine Mincle/Mcl (Zhao et al., 2014).

The role of Mincle in mycobacterial infections is controversial, as it has been shown to be important for controlling *M. bovis* BCG infection (Behler et al., 2015; Behler et al., 2012), but not to be essential for controlling Mtb infection in mice (Heitmann et al., 2012). Where Mincle is localized is also controversial, and whether it relocalizes during mycobacterial infection is not clear. A better understanding of Mincle, the potential interaction with mycobacteria and where this interaction take place might help elucidate the role of Mincle during mycobacterial infections.

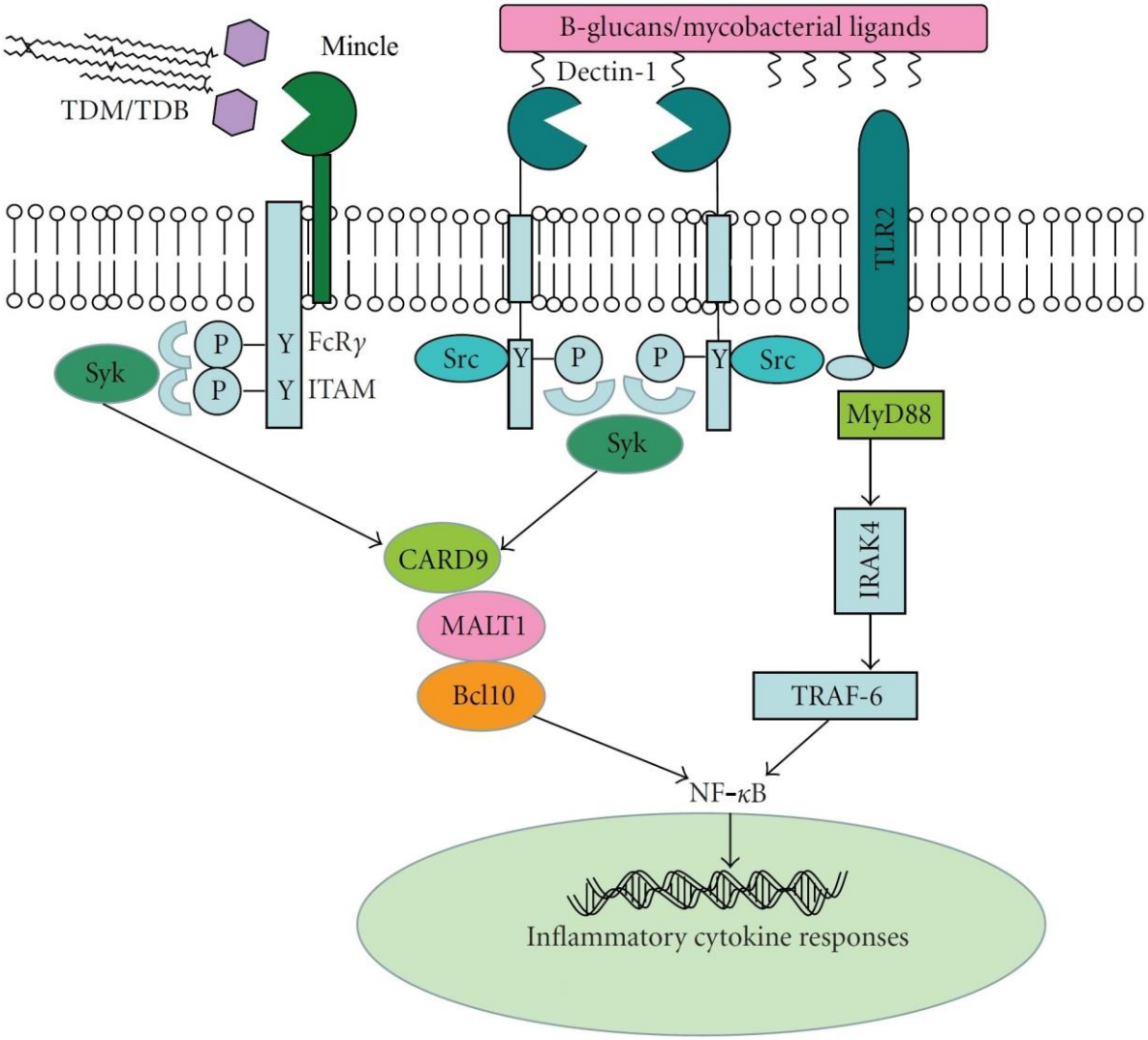

Figure 1.4 Simplified illustration of signalling from receptors involved in mycobacterial recognition. For Mincle, FcRγ-association is mediated by a positively charged arginine in the transmembrane region (Yamasaki et al., 2008). Mincle is presented here as a representative of CLRs from the Dectin-2 group; Mcl and Dectin-2 also signal through CARD9, possibly through heterodimerization. Signalling pathways from CLRs independent of CARD9, e.g. through Raf-1 or MAPK have also been reported (Dambuza and Brown, 2015), but are not shown here. Adapted from (Marakalala et al., 2011).

2 Aims and objectives

The prevalence of NTM-diseases caused by opportunistic pathogens such as MAC is increasing and has now surpassed TB in developed countries (Daley and Griffith, 2010; Prevots et al., 2010). The role of Mincle, a receptor for mycobacterial glycolipids, in mycobacterial infection has been reported controversially, and no studies emphasizing on the role of Mincle in *M. avium* infection have been published yet. Not much is known about the exact mechanisms and kinetics in *M. avium* infection and where Mincle is localized in macrophages during mycobacterial infection. Sorting out the potential trafficking of Mincle in an infection model using *M. avium* could help elucidate the role of Mincle in mycobacterial infection.

Objectives for this study:

- Investigate the role of the C-type lectin receptor Mincle during *M. avium* infection:
    - Do comparative infection studies using a murine *in vitro* model to test whether WT and Mincle-deficient BMMs differ in their ability to phagocytose and/or kill *M. avium* or differ in secretion of cytokines associated with mycobacterial infection.
- To be able to characterize where Mincle is localized in macrophages/dendritic cells during infection with *M. avium*. To get there, we want to establish tools for localization studies of Mincle by
    - Testing potential antibodies for confocal microscopy imaging
    - As an alternative strategy, establish a model for overexpression of Mincle and/or other CLRs with the potential of using tagged constructs.
    - If possible, use this model in infection studies.

3 Experimental methods

General laboratory work

All working procedures including living mammalian and mycobacterial cells were performed under sterile conditions in class II biological safety cabinets (Esco Labculture®, LA2-K). Standard operating procedures (SOPs) were followed, and sterile techniques were practiced thoroughly throughout.

Table 3.1 Common reagents, abbreviations and providers.

Reagent	Abbreviation	Provider
Dulbecco's Phosphate Buffered Saline	PBS	Sigma Aldrich Life Sciences
Dimethylsulphoxide	DMSO	Sigma Aldrich Life Sciences
Penicillin Streptomycin	PenStrep	Sigma Aldrich Life Sciences
Dulbecco's Modified Eagle Medium	DMEM	
Fetal bovine calf serum (heat inactivated)	FCS	Gibco Life Technologies
HEPES Buffer Solution (1M)	HEPES	Gibco Life Technologies
Roswell Park Memorial Institute 1640 medium	RPMI	Sigma Aldrich Life Sciences
Hank's Balanced Salt Solution	HBSS	Sigma Aldrich Life Sciences
L929-conditioned medium	L929	In-house preparations
Recombinant granulocyte-macrophage colony-stimulating factor (carrier-free)	rGM-CSF	BioLegend
Bovine serum albumin	BSA	Sigma Aldrich Life Sciences
Enriched Middlebrook 7H9 medium	7H9	Becton Dickinson; BD
Opti-mem® I (1x) Reduced serum medium	Optimem	Gibco Life Technologies

Before usage, RPMI and DMEM were added L-glutamine (to a final concentration of 100 µg/ml). In addition, HEPES was added to the RPMI medium (final concentration 10 mM).

3.1 Isolation and differentiation of primary cells

3.1.1 Isolation and freezing of bone marrow (BM) cells

C57BL/6 mice acquired from NTNU/St. Olavs Comparative Medicine Core facility were euthanized using CO^2 and generously sprayed with ethanol (70 %). Both hind legs (2 x femur and 2 x tibia) were dissected out and placed in ice-cold HBSS. After removal of remaining connective tissue, the rinsed whole bones were placed in ethanol (96 %) for 1 min. Epiphyses were cut off as close to the end as possible, and bones were flushed from both sides using a syringe with a 0.5 mm needle (5 – 10 ml HBSS per bone) and fluids collected. The BM cells were spun down (1500 RPM / 43 *g*, 5 min) and supernatant discarded. BM cells were gently resuspended in RPMI to a concentration of 8 – 12 x 10^6 cells/ml, and aliquoted in cryovials, 500 µl in each.

Freezing medium (2x; 20 % DMSO, 80 % FCS, 500µl) was added to each cryovials, to a final concentration of 4 – 6 x 10^6 BM cells/vial in 1 ml of freezing medium (50 % RPMI, 40 % FCS, 10 % DMSO). Content was gently mixed by tilting the cryovials, then A) immediately put in a Mr. Frosty™ cryo-box and placed in -80 ^oC, then transferred to liquid nitrogen the next day, or B) put directly in liquid nitrogen.

Mincle-deficient ($Clec4e^{-/-}$) BM cells (C57BL/6J background) were generously provided by Christine A. Wells, generated as previously described (Wells et al., 2008).

3.2 Thawing and differentiation of BM cells to BMMs or BMDCs

Differentiating medium to form BMMs: RPMI, 10% FCS, 20 % L929.
Differentiating medium to form BMDCs: RPMI, 10 % FCS, rGM-CSF (10 ng/ml).

BM cells were flash-defrosted in a water bath (37 ^oC). Once thawed, differentiation medium (1 ml) was added to the cryovial, and content (now 2 ml) dispersed in warm differentiation medium (8 ml, 37 ^oC) in a petri dish (Ø = 10 cm). The cells were incubated (5 % CO_2, 37 ^oC) in an incubator (Forma Steri-cycle, Thermo Scientific). After 3 days, 5 ml old medium was removed and 5 ml fresh differentiation medium added (37 ^oC). After 5 – 6 days of differentiation, the cells were gently scraped off, spun down (1500 RPM, 4 min) and resuspended in RPMI/10 % FCS. Differentiated BMMs/BMDCs were grown in RPMI/ 10 % FCS for further experiments.

3.2 Quantitative reverse transcription real-time polymerase chain reaction (RT-qPCR)

To measure the gene expression levels of Mincle, mRNA levels were measured by RT-qPCR.

RNA isolation

Cells grown in a 24-well plate (200 000 cells/well, 2 wells per condition) were rinsed with PBS before RLT lysis buffer (350 µl, 1 % β-mercaptoethanol) was added to each well. RNA was purified using a QIAcube instrument and RNeasy mini kit (both Quiagen), using the program "RNA mini for animal cells and tissue with DNAse". Purity and concentration of isolated RNA was measured using NanoDrop ND-1000 (Saveen Werner).

cDNA synthesis

cDNA was synthesized using "High capacity RNA-to-cDNA" kit (Applied Biosystems) and procedure followed. A 2720 Thermal cycler (Applied Biosystems) was used for reverse transcription.

qPCR

cDNA samples were diluted to 1 ng/µl in DNAse-free water, assuming that all RNA was reverse transcribed to cDNA. TaqMan primers/probes were used in combination with 2xPerfecta® qPCR FastMix buffer (Quanta Biosciences) and diluted cDNA (1, 10 and 9 µl, respectively). The setup was based on technical triplicates, with water-controls for each gene. GAPDH was chosen as an internal reference gene. A StepOnePlus instrument (Applied Biosystems) was used for PCR cycling, and following analysis was done using the StepOne software (Applied Biosystems). Relative quantification/fold change induction relative to untreated samples was estimated using the $2^{-\Delta\Delta Ct}$ method.

3.3 *M. avium* maintenance and preparation for infection

Virulent *M. avium* (strain 104 pMH109 C) expressing either firefly luciferase or cyan fluorescent protein (CFP) was used in all infection-experiments. Mycobacteria were cultured in enriched Middlebrook 7H9 medium (table 3.2) under agitation (37 ^{o}C). To freeze down bacteria, *M. avium* were grown in 7H9 medium to an optical density (OD) ≥ 0.6, and sterile glycerol added to a final concentration of 20 %, before aliquoted (0.7 – 1 ml) in cryotubes and placed in a freezer (- 80 ^{o}C). Filter tips were used in all work involving *M. avium*.

Table 3.2. Enriched Middlebrook 7H9 medium

Reagents	Amount in 500 ml	Manufacturer
Middlebrook 7H9 in 450 ml sterile water	2.35 g	Difco/Becton Dickinson
Sterile glycerol (85 %)	1 ml	Merck Millipore
20 % Tween 80	1.25 ml	Sigma Aldrich Life Sciences
Albumin-dextrose catalase (ADC) enrichment	50 ml	Sigma Aldrich Life Sciences

3.3.1 Infection

Mycobacteria in early logphase (OD600 = 0.3-0.6) were used for infection. Mycobacteria were rinsed in PBS twice: Mycobacteria in 7H9 medium (1 ml) was spun down in microtubes with screw lid (10 000 rpm, 4 min). 7H9 medium was discarded without disturbing the mycobacterial pellet before resuspension in PBS (1 ml). Bacteria were spun down again, and resuspended in PBS (1 ml). To remove any clumping of mycobacterial cells, the cells were sonicated and vortexed (3 x 30 sec), then passed through a 0.5 mm needle three times. OD600 was measured after rinsing to calculate the number of bacteria (OD600: 1.0 = 4.5 x 10^8 bacteria/ml).

A multiplicity of infection (MOI) of 10 was used in all infection experiments unless otherwise stated. Plating of inoculum (triplicates, serial dilutions) on Middlebrook 7H10 plates (BD) and subsequent counting after 7 – 9 days of incubation (37 ^{o}C) was done as a control for OD measurements in all experiments. Plates were kept in sealed plastic bags to avoid drying.

Unless for confocal imaging purposes, BMMs that were infected were grown in 96-well plates, (20 000 BMMs per well, 100 µl RPMI/10 % FCS), and 3 wells per condition, also for uninfected

controls. When infecting the cells, 50 µl of old medium was removed, and 50 µl medium ±*M. avium* were added. For time points > 4 h post infection, medium was changed after 4 h, also for uninfected controls. 70 µl of the medium was replaced with fresh medium every second day.

As positive controls for later ELISA measurements, non-depleted zymosan (30 µg/ml), a ligand for Dectin-1 and TLR 2, or K12-derived LPS (TLR 4 ligand, 100 ng/ml) were used. Supernatant from infected cells and positive/negative controls was frozen down (-20 ^{o}C) for later ELISA measurements.

3.3.2 Colony-forming units of *M. avium*

As a control for the luciferase assay (section 3.4), lysate from infected BMMs were plated on 7H10 plates and cultured for 7 – 9 days before counting of mycobacterial colonies.

Infected and uninfected cells were lysed in 120 µl lysis buffer (1x, from "Passive lysis buffer, 5x", Promega, diluted in sterile water). Lysate (10 µl) from wells undergoing the same treatment were pooled (30 µl in total, three wells per condition), before several dilutions were made (PBS). Plating was done either by plating droplets of several dilutions (10^{-1} – 10^{-5}, 2 x 5 µl) or by smearing diluted lysate (100 µl) on 100 mm 7H10 plates. Estimation of *M. avium* per BMM was done using the lowest countable dilutions, assuming the number of BMMs was stable.

3.4 Luciferase assay

Infected and uninfected cells were lysed in 120 µl lysis buffer (1x, from "Passive lysis buffer, 5x", Promega, diluted in sterile water). Lysate were transferred to an OptiPlate™-96 (PerkinElmer), in technical duplicates á 50 µl. Luciferase substrate (50 µl, Promega) was added to the lysate, and luminescence from luciferase activity was measured after 5 min using a Wallac Victor^3 1420 multilabel counter (PerkinElmer). Exposure time was 1 second per well, and values obtained from the Victor^3 counter was counts per second (CPS). Absolute quantification of *M. avium* was not done, measurements were used for relative comparison of the different samples.

3.5 Measurement of secreted cytokines by ELISA

Cytokines secreted by BMMs were measured by ELISA (Enzyme-linked immunosorbent assay). Kits (DuoSet, R&D Systems) were used, and procedures followed. Samples added were diluted 1:2.5. TMB (A+B) solution (BioLegend) was used as substrate for the horseradish peroxidase. An iMark™ Microplate Absorbance Reader (Bio-Rad) was used for measurements.

Absorbance was read at 450 nm, subtracting 570 nm to correct for potential differences in plastic ware. For all measurements, a logit-log function was chosen to make the standard curve. Values obtained were trusted down to the lowest standard concentration. For high values, cut-off points were adjusted manually, and trusted only within the more linear range of the standard curve to avoid uncertain extrapolation.

3.6 Antibody-staining of cells.

Different staining procedures were followed, listed below. Unless otherwise stated, the procedures were done in room temperature. After fixation, staining was done outside of the biosafety hood (non-sterile).

Table 3.3 Primary and secondary antibodies used.

Antibodies	Species/specificity	Dilutions used	Original conc. (mg/ml)
Wells' Ab	Rabbit	1:50 and 1:100	0.43
α-mMincel (4A9; MBL)	Rat	1:100	1
α-hMCL (9B9; BioLegend)	Mouse	1:100	0.5
α-hMincle (6782A; IMG)	Rabbit	1:100	0.5
α-HA (16B12; BioLegend)	Mouse	1:500	1
Alexa-405 (Invitrogen)	α-mouse	1:1000	2
Alexa-405 (Invitrogen)	α-rabbit	1:1000	2
Alexa-488 (Life Technologies)	α-mouse	1:1000	2
Alexa-488 (Life Technologies)	α-rabbit	1:1000	2
Alexa-555 (Life Technologies)	α-rabbit	1:1000	2
Alexa-555 (Life Technologies)	α-rat	1:1000	2
Alexa-647 (Life Technologies)	α-rabbit	1:1000	2
Alexa-647 (Invitrogen)	α-rat	1:1000	2
Alexa-647 (Invitrogen)	α-mouse	1:1000	2

3.6.1 Confocal staining procedures

Paraformaldehyde (PFA) fixation and staining

Cells were fixed using PFA (2 %, 15 min) and washed (PBS, 3 x 5 min) before blocking (PBS, 10 % FCS, 0.05 % saponin, 1h). Primary antibodies were added in FACS buffer (PBS, 2 % FCS, 0.05 % saponin). After 1h, the cells were washed (FACS buffer, 3 x 5 min) and secondary antibodies* added (FACS buffer, 10 min). The cells were washed (PBS + nuclear stain (DRAQ5, 1:1000), 2 x 5 min, then 5 min in PBS), then left in PBS (4 ^{o}C) until imaging.

*Secondary antibodies were anti-mouse/rat/rabbit conjugated to Alexa-405/488/555/647, depending on the primary Ab used and/or the presence of other fluorochromes. For details, see table 3.3

Methanol-acetone fixation and staining

Same procedure as for PFA-fixed cells, except: methanol/acetone (1:1) was used for fixation (-20 ^{o}C, 5 min), and instead of FACS buffer, (PBS, 2 % FCS) was used.

3.6.2 Staining for flow cytometry

Cells were fixed using PFA (2 %, 20 min, 4 ^{o}C) and washed (PBS, 2 % FCS, 2 x 5 min). Fc Block (HuFcR, eBioscience) was added (1:200, in FACS buffer, 5 min) before primary antibodies were added directly (2 x concentration, in FACS buffer, 2h, 4 ^{o}C). Cells were washed (FACS buffer, 2 x 5 min) before secondary antibodies were added (in FACS buffer, 15 min, 4 ^{o}C). The cells were washed again (FACS buffer, 2 x 5 min, 4 ^{o}C) before they were analysed by flow cytometry.

3.7 Confocal microscopy

Before imaging, cells were grown in glass bottom dishes (35 mm, MatTek) or in 8-well multi-chambers (Nunc/Thermo Fisher Scientific), and stained as described in section 3.6.1. For HEK293 cells, poly-L-lysine-coated multi-chambers were used.

All images presented in this study were taken using Zeiss LSM 510 Meta FCS with objective 63 x 1.4 Oil DIC (Zeiss). If overlapping emission curves could be expected, different tracks were used to reduce the noise. Laser intensity and gain was kept identical when comparing samples (exceptions were made if re-imaging was done at later time points, then the gain was increased somewhat to compensate for loss in intensity). Unless otherwise stated, images in this study are presented as compressed Z-stacks of 4 slices, done in the software ImageJ using the

function “Z-project” and “sum slices”. Gain and brightness/contrast was adjusted to show some background noise in all images on purpose, to present the data in an honest way.

Comparing the phagocytic uptake of *M. avium* in WT and Mincle$^{-/-}$ BMMs

While imaging, the CFP-channel was off when choosing field of view. Z-stacks were obtained, and the number of *M. avium* taken up was counted manually. To avoid biased counting (it was not always clear if it was one or two bacteria), the file names were edited by a fellow student, Camilla Wolowczyk, and the key was given after counting was done.

3.8 HEK293 cell line maintenance

HEK293 cells were grown in T-75 culture flasks in DMEM, 10 % FCS, 1 % PenStrep (37 ºC, 8 % CO_2). Cells were passaged (1:20) at about 80 % confluency, twice a week. When used in experiments, cells were cultured in DMEM, 10 % FCS.

3.9 Plasmid amplification and isolation

The various constructs of human and murine CLRs used for overexpression (table 3.4) had previously been cloned into the MigR1 backbone by Jenny Ostrop (Ostrop, 2015).

Plasmid amplification was done using *Escherichia coli* DH5α, and plasmids were isolated using Qiagen Maxiprep kit (Qiagen).

3.9.1 Bacterial transformation and plasmid amplification

Competent *E. coli* DH5α was thawed on ice, aliquoted (25 µl) in 1.5 ml Eppendorf tubes and DNA added (5 µl, 50 ng). The cells were incubated with the DNA on ice for 30 minutes, heat-shock transformed (42 ºC, 45 seconds) and rested on ice for 2 minutes. Pre-warmed LB-medium (37 ºC, 180 µl) was added to the tubes and bacteria cultured without antibiotics (1h, 37 ºC) before plating (70 µl) on LB-plates with ampicillin (Amp, 100 µg/ml). The plates were incubated overnight (37 ºC) and clones picked the following day (plated untransfected controls did not show any bacterial colonies). Selected colonies were cultured in LB medium (100 ml, Amp 100 µg/ml) until the next day (37 ºC, 250 RPM) before plasmid isolation was done using a maxiprep-kit (Qiagen).

3.9.2 Plasmid isolation

Plasmid isolation was done using Qiagen EndoFree® maxiprep-kit (Qiagen). The protocol is shown in appendix IV and was followed except for the following:

- Before filtering the lysate (between step 5 and 6), lysed bacteria were spun down (2280 *g*, 10 min) to get rid of excessive cell debris.
- Step 12: Eluted DNA was spun down at 2280 *g*, 4 ºC, for 90 min.
- Step 13: Washed DNA was spun down at 2280 *g*, 4 ºC, for 40 min.

Table 3.4 Plasmids used in this study. All plasmids were provided by Jenny Ostrop.

Description	Back bone	Back-bone size (kb)	Insert	Insert Size (bp)	Ab res.	Bacteria
Mouse FcRgamma chain, cloned in NT Zeocin via Xba1, Sac1	NT Zeocin	?	mFcεR1	~100	Amp	DH5α
pCL-Eco packaging vector for retroviral transduction together with Migr1 (murine)	CMV-LXSN	4.5	gag/pol/env	-	Amp	DH5α
MigR1 empty vector	MigR1	6.2	empty vector	-	Amp	DH5α
human CLEC4D/MCL, cloned in MigR1 via BglII	MigR1	6.2	hCLEC4D/ hMCL	~700	Amp	DH5α
human CLEC4E/MINCLE, cloned in MigR1 via BglII	MigR1	6.2	hCLEC4E/ hMINCLE	~700	Amp	DH5α
mouse Clec4d/Mcl, cloned in MigR1 via BglII	MigR1	6.2	mClec4d/ mMCL	~700	Amp	DH5α
mouse Clec4e/Mincle, cloned in MigR1 via BglII	MigR1	6.2	mClec4e/ mMincle	~700	Amp	DH5α
mouse Clec4e/Mincle, HA-tag C-terminus, cloned in MigR1 via BglII	MigR1	6.2	mClec4e-HA	~700	Amp	DH5α

3.10 Transcient transfection using Gene Juice reagent

HEK293 cells were seeded out in 24-well plates the day before transfection (100 000 cells/well, in 0.5 ml DMEM, 10 % FCS, 1 % PenStrep). Preparations made per well:

Gene Juice® Transfection reagent (1.5 µl) were added in Optimem medium (25 µl) and vortexed. After 5 min, plasmids were added (0.25 µg FcRγ + 0.25 µg empty vector or CLR of interest) and solution vortexed and spun down. After 10 min, the solution was added to the cells. The cells were incubated (37 ºC, 8 % CO_2) until next day before staining and further

analysis was done. If other cell numbers than listed above were transiently transfected, volumes were up/downscaled, and ratio kept.

3.11 Flow cytometry

Cells were transiently transfected and stained as previously described (3.10 and 3.6.2, respectively). Measurements were obtained using FACSCanto™ II flow cytometer (BD Biosciences), and the software FACSDiva. Further analyses were done using the software FlowJo (v.10.1). Expression of green fluorescent protein (GFP) was used as a control for transfection, and for CLR-staining, secondary antibodies linked to Alexa-647 was used. Hence, no compensation for spectral overlap was performed. Gating was done to exclude duplets (FSC-H vs FSC-A). Comparable cell populations were obtained by "tight" gating of the main population (SSC-A vs FSC-A), and this procedure was applied if FSC-H was not recorded to reduce the risk of including duplets.

3.12 Retroviral transduction of primary BMMs and BMDCs

Only the optimized procedure is presented. All work restricted to the virus lab was done by my co-supervisor Jenny Ostrop.

Day 1: Phoenix Eco cells were seeded out in 6-well plates (200 000 cells/well, in DMEM, 10 % FCS, 2 ml).
Day 2: The Phoenix Eco cells were transiently transfected (see section 3.10) with an empty vector or CLR of interest and FcRγ, together with the pCL vector (1:1:1) to make virus particles, as described by (Naviaux et al., 1996).
Day 4: Successful transfection was confirmed using a fluorescent microscope. Supernatant, now containing virus particles, was collected from the Phoenix Eco cells and filtered (0.45 µm). Filtered supernatant (1 ml/well) was added to still differentiating (2 days after thawing) BMM/DCs grown in 12-well plates (~ $1x10^6$ cells/well), and the plates were spun down (1500 RPM, 2h, 37 ^oC). The BMM/DCs were rested (2h, 37 ^oC) and medium changed (2 ml).
Day 8: BMM/DCs were transferred to confocal dishes, and LPS added (10 ng/ml) to increase adherence to the glass surface.
Day 9: Cells were fixed (2 % PFA, 20 min) before further staining and imaging was conducted.

4 Results

4.1 Comparison of WT and Mincle$^{-/-}$ BMMs in response to *M. avium* infections

Previous comparative infection studies of WT and Mincle-deficient mice using whole bacteria have shown that bacterial growth restriction of *M. bovis* BCG was Mincle-dependent (Behler et al., 2012), while Mincle was shown to not be essential for controlling infection with *M. tuberculosis* (Heitmann et al., 2012). Hence, the importance of Mincle seem to differ in regard to mycobacterial species causing infection. Given the widespread and increased occurrence of MAC infections (Brode et al., 2014), we wanted to investigate whether the absence of Mincle affected the capability of BMMs to phagocytose and/or kill *M. avium*.

4.1.1 Establishment of methods and controlling the cells used

Before side-by-side experiments of WT and Mincle$^{-/-}$ BMMs were conducted, methods were tested, confirmed and optimized using WT BMMs, and levels of Mincle mRNA were measured in WT and Mincle$^{-/-}$ BMMs.

Freezing and thawing of BM cells

Two different freezing procedures of freshly isolated BM cells were tested, both using the same cryopreservative solution. For method A, cryovials were put in a Mr Frosty™ (cryobox with isopropanol) and placed in a -80 ^{o}C freezer, then transferred to liquid nitrogen the next day. For method B, cryovials were placed directly in liquid nitrogen. Viability of the flash-defrosted cells were measured after 5 days of differentiation and showed 95 % and 5 % viability for method A and B, respectively. Method A was used thereafter.

WT BM cells were isolated from C57BL/6-mice as described in section 3.1, while Mincle-deficient BM cells (C57BL/6J background) were generously provided by Christine A. Wells.

Mincle mRNA is upregulated in response to LPS in WT BMMs

Mincle has previously been shown to be upregulated in macrophages in response to LPS (Matsumoto et al., 1999). To test whether this was observed in the WT BMMs used in this study, and to confirm the genotype of the Mincle$^{-/-}$ cells, mRNA levels of Mincle were measured by RT-qPCR.

WT and Mincle$^{-/-}$ BMMs were stimulated with LPS overnight (10 or 100 ng/ml) or kept unstimulated. Levels of Mincle mRNA were measured and found to be induced in response to LPS in WT BMMs, while no Mincle mRNA was detected in Mincle$^{-/-}$ BMMs (fig. 4.1).

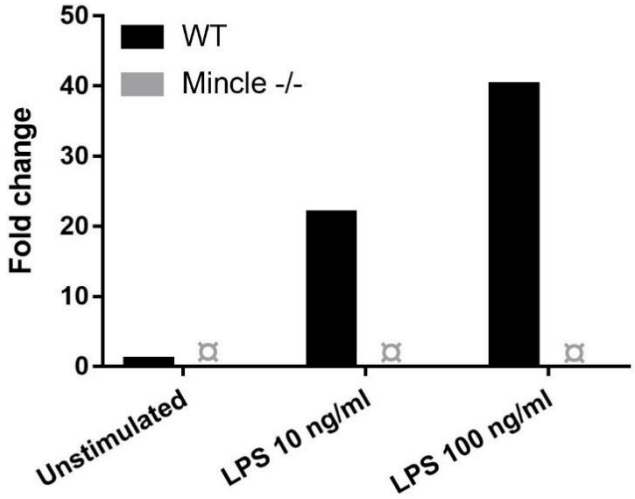

Figure 4.1 Mincle is upregulated in WT BMMs in response to LPS. Mincle mRNA in WT and Mincle$^{-/-}$ BMMs in response to LPS stimulation was measured by RT-qPCR. Fold change relative to unstimulated WT BMMs, using GAPDH as an internal reference gene is shown. Data are based on one experiment, with two wells per condition and technical triplicates. ¤ = CT-value undetermined. Baseline- and threshold settings for the analysis done can be found in appendix I.

4.1.2 WT and Mincle-deficient BMMs do not differ in their ability to phagocytose or kill *M. avium*

WT and Mincle$^{-/-}$ BMMs were infected with luciferase-expressing (luc^{+}) *M. avium* (MOI 10) to investigate whether they differed in uptake and/or killing of the bacteria. The experiment was repeated four times, and no differences were observed between WT and Mincle$^{-/-}$ BMMs, neither at early nor late (30 min – 5 days) time points (fig. 4.2A). Uninfected controls showed no luciferase activity (data not shown).

Laser scanning confocal microscopy was used as a method confirmation for the luciferase assay and to compare the phagocytic uptake of *M. avium* in WT and Mincle$^{-/-}$ BMMs. Cells were infected with cyan fluorescent protein-expressing (CFP^{+}) *M. avium* (MOI 10), and the number of bacteria taken up by the BMMs was counted manually. No differences were observed between WT and Mincle$^{-/-}$ BMMs regarding the number of *M. avium* taken up per cell or the percentage of BMMs that had phagocytosed at all (fig. 4.2B). Uptake of bacteria during the first 24 hours resembled the pattern observed in the luciferase assay. Example images show phagocytosed *M. avium* (fig. 4.2C and D).

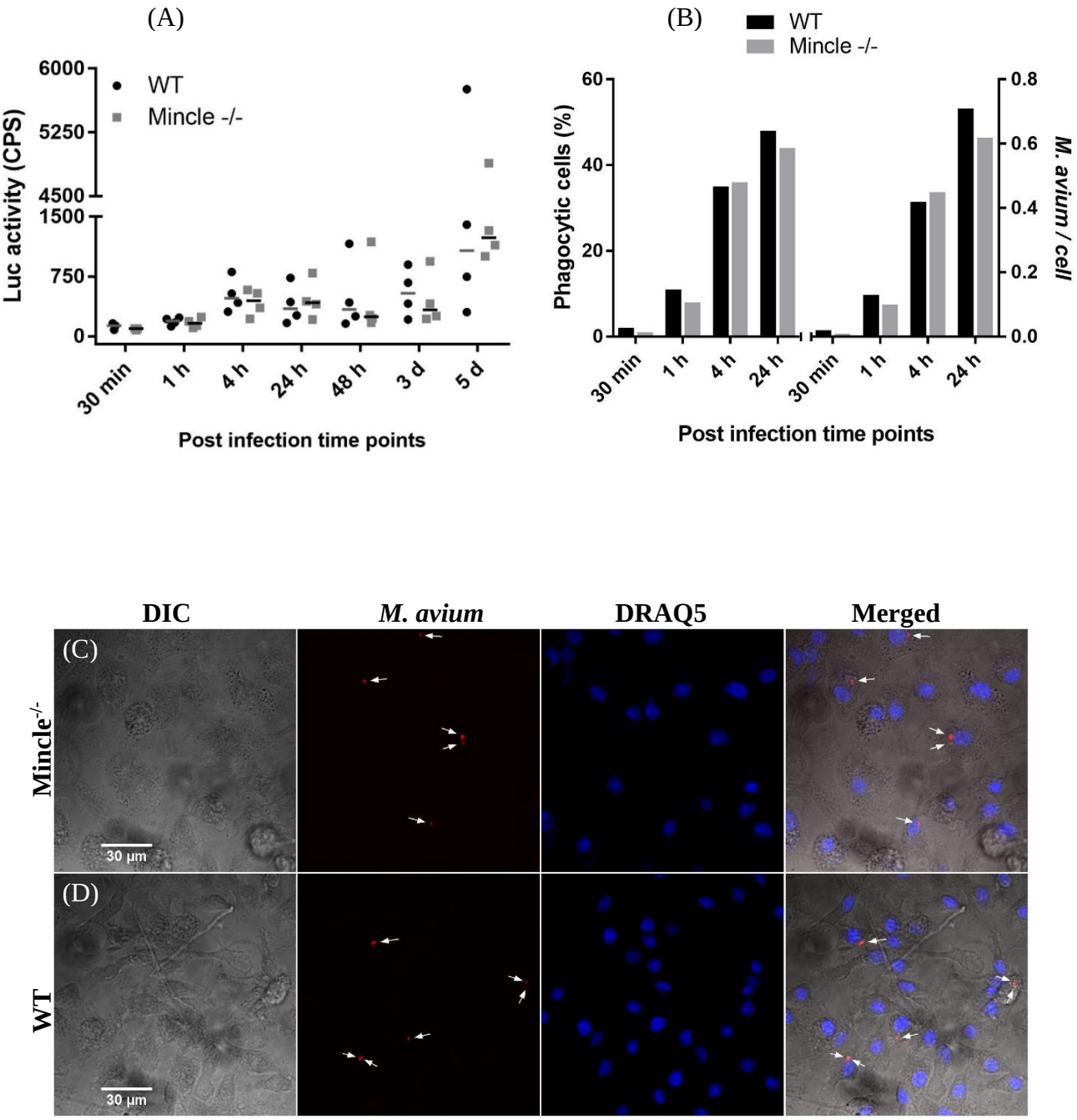

Figure 4.2 Uptake and killing of *M. avium* in WT and Mincle$^{-/-}$ BMMs.
A) Luciferase activity (counts per second, CPS) of lysate from BMMs infected with luc^{+} *M. avium* were measured at different time points. Each data point in the figure represents an independent experiment, and lines represents the median of the four different experiments.
B) Uptake of *M. avium* based on confocal microscopy and manual counting. Bars presented are the mean from one experiment, with 100 – 115 cells per condition.
Example images (compressed Z-stack of 10 images) of phagocytosed *M. avium* is shown for fixed Mincle$^{-/-}$ (C) and WT (D) BMMs, 4 hours after infection. White arrows indicate phagocytosed *M. avium*.

As a method confirmation of the luciferase assay, lysate from WT and Mincle$^{-/-}$ BMMs infected with *M. avium* (MOI 10) were plated on 7H10 plates and the number of bacterial colonies counted after 7 – 9 days of incubation.

A preliminary colony-counting experiment indicated a difference in killing of *M. avium* between WT and Mincle$^{-/-}$ BMMs (data not shown). The experiment was repeated three times, using two different plating techniques; dilution series à 5 µl droplets ("spotting") and smearing of diluted 100 µl lysate on 100 mm 7H10 plates ("full plate"). Estimation was done using the lowest countable dilutions, around 40 – 80 and 200 – 500 colonies for spotting and full-plate experiments, respectively. No differences were detected between WT and Mincle$^{-/-}$ BMMs regarding the killing of phagocytosed *M. avium* (fig. 4.3). No bacterial colonies were observed in uninfected controls (data not shown). Patterns observed from these experiments resembled the patterns from luciferase assays, thereby supporting the luciferase-based method.

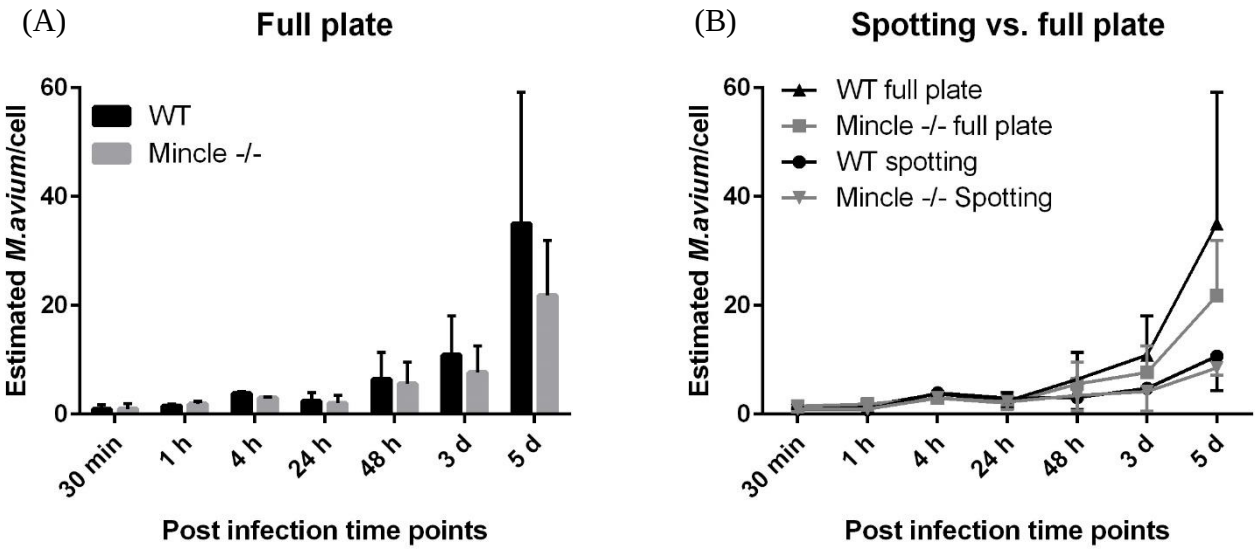

Figure 4.3 Survival of *M. avium* in infected WT and Mincle$^{-/-}$ BMMs.
A) Estimated live *M. avium* per BMM, based on colonies formed 7 – 9 days after plating of 100 µl diluted lysate on 100 mm 7H10 plates from infected BMMs. Bars represent the mean and standard deviation (SD) of three experiments.
B) Comparison of a full-plate (100 µl lysate, smeared over a 100 mm 7H10 plate) and a spotting technique (5 µl droplets of lysate) and subsequent estimation of live *M. avium* per BMM.

4.1.3 LPS-priming does not alter the phagocytic- or killing capacity of BMMs infected with *M. avium*

Priming BMMs with LPS has been shown to upregulate the expression of Mincle (Matsumoto et al., 1999), also confirmed in this study (section 4.1.1). To assess whether boosting Mincle expression could reveal any differences regarding the uptake and/or killing of *M. avium*, BMMs were primed with LPS (10 ng/ml) overnight. LPS-primed and unprimed WT and Mincle$^{-/-}$ BMMs were infected with luc^{+} *M. avium* (MOI 10) and the levels of *M. avium* were measured by luciferase assays.

Unprimed BMMs indicated no difference between WT and Mincle$^{-/-}$ in the uptake or killing of *M. avium* (fig. 4.2A). Priming BMMs with LPS did not alter phagocytic activity or killing of *M. avium*. The alikeness regarding phagocytosis and killing of *M. avium* by LPS-primed, unprimed, WT and Mincle$^{-/-}$ BMMs is shown (fig. 4.4). Uninfected controls showed no luciferase activity (data not shown).

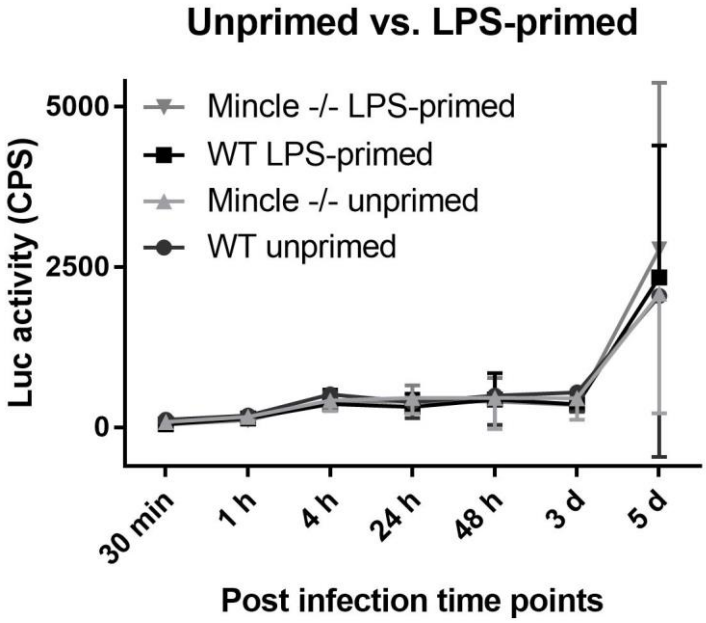

Figure 4.4 Luciferase assays of LPS-primed and unprimed BMMs. Luciferase activity (counts per second; CPS) measured from lysate of WT and Mincle$^{-/-}$ BMMs infected with luc^{+} *M. avium* (MOI 10), either LPS-primed (10 ng/ml overnight, prior to infection) or unprimed. Data points represent the mean and SD of three separate experiments with three wells per condition.

4.1.4 Mincle does not affect the secretion of IL-6, G-CSF, KC or IP-10 in BMMs infected with *M. avium*

Selected cytokines associated with CLR-engagement and mycobacterial infections were measured to test whether Mincle$^{-/-}$ BMMs responded differently during *M. avium* infection than WT. G-CSF, KC, IP-10 and IL-6 secreted by BMMs infected with *M. avium* (MOI 10) were measured using ELISA. Secreted IP-10 was below the lowest standard in all conditions, as was the levels of secreted cytokines for uninfected controls (data not shown). The cytokines measured indicated no difference between WT and Mincle$^{-/-}$ BMMs in response to *M. avium* (fig. 4.5).

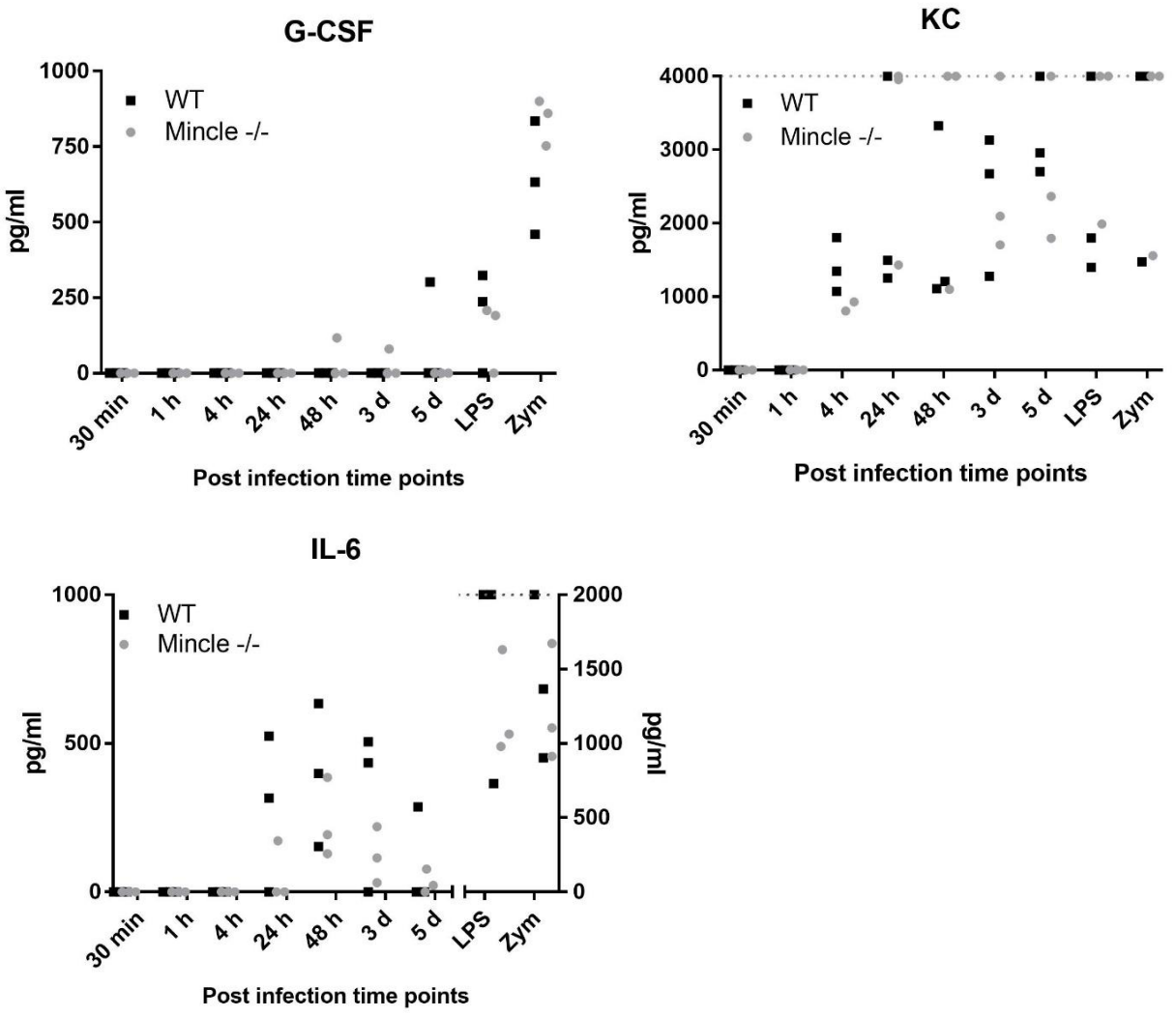

Figure 4.5. Secreted G-CSF, IL-6 and KC from WT and Mincle$^{-/-}$ BMMs infected with *M. avium*. Each data point represents an experiment with three wells per condition. For values that exceeded the standard, data points are shown as dots along the highest trustable values. That is, true values ≥ 2000 or 4000 pg/ml for IL-6 and KC, respectively. Positive controls to the right of the x-axis break (IL-6) are plotted on the right y-axis. Uninfected, positive controls were added LPS (100 ng/ml) or zymosan (30 µg/ml) and cell culture supernatant were collected after 24 hours of stimulation.

In summary, data from these comparative *in vitro* experiments suggest a non-essential role for Mincle regarding BMMs' capability to phagocytose and kill *M. avium*, or secretion of G-CSF, IL-6, KC or IP-10 in response to *M. avium* infection.

4.2 Establishing tools to study the localization of Mincle

Not much is known about the exact mechanisms and kinetics in *M. avium* infection and where Mincle is localized in macrophages during mycobacterial infection. Most studies regarding Mincle localization have used flow cytometry for determination, distinguishing only between intracellular- and surface localization. Some have used confocal microscopy to study Mincle localization, (e.g. Wells et al. 2008), but none have shown co-localization with proteins of known localization. Microscopy would therefore be a valuable tool in infection studies.

Therefore, we further sought to establish tools to better be able to study the localization of Mincle in primary BMMs and BMDCs, results are presented in the following sections.

4.2.1 Antibody-testing using flow cytometry and confocal microscopy

Due to sequence-similarities in their ectodomains (Furukawa et al., 2013), Mincle and Mcl were thought to be the most likely candidates for cross-reactivity of the antibodies, and both human and murine versions were included when testing for antibody specificity. HEK293 cells were transiently transfected with the CLR of interest and murine FcεRI-γ (FcRγ) in a 1:2 ratio (µg DNA) and an empty vector was included as a control. Antibodies tested were 4A9 and Well's Ab (both α–mMincle), an antibody against an HA-tag (α-HA), as well as an α-hMINCLE (IMG) and an α-hMCL (9B9) Ab. Intracellular- and surface staining was done and samples measured using flow cytometry.

Representative examples for gating of singlets, live and transfected cells are shown in fig. 4.6. Constructs of murine Mincle linked to the widely used hemagglutinin (HA) tag in combination with an α-HA antibody was included as a positive control. Gating examples of antibody-stained cells are shown in fig. 4.7, while remaining data is shown more condensed in fig. 4.8.

In the MigR1-plasmid used, GFP followed the gene of interest after an IRES for bicistronic protein expression. Fig. 4.7 shows cells gated on double positives; i.e. GFP and HA positive cells. To test whether any cells expressed the CLR of interest, but not GFP, gating was done directly on live singlets using the SSC-A vs. APC-A parameters. For that particular transfection (intracellular staining), 75 % of live singlets were HA positive, compared to 37 % GFP positive, demonstrating that the correlation could be imperfect. In order to test for antibody specificity, double positives were used.

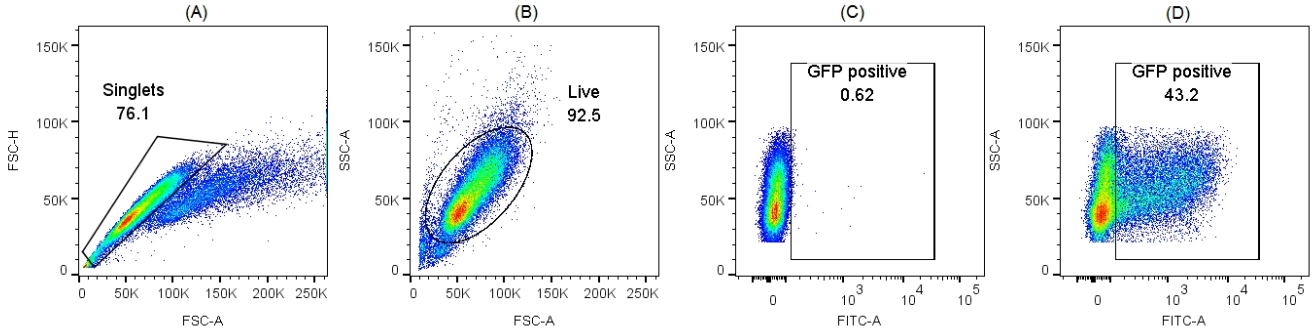

Figure 4.6 Gating examples and transfection efficiency of HEK293 cells.
A) Example of gating done to select singlets and exclude duplets. B) Gating example to select live cells. C) Gating example done using untransfected cells. D) Same gating as in (C), now showing GFP positive transfected cells.

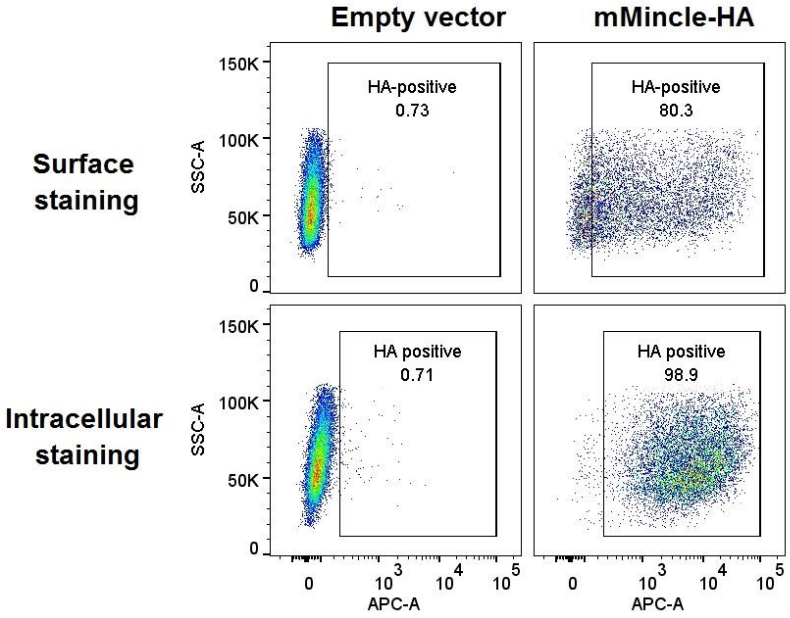

Figure 4.7 Gating examples for antibody-stained cells. HEK293 cells transfected with an empty vector or a construct of mMincle linked to an HA-tag were stained with an α–HA Ab using procedures for surface- and intracellular staining. Previous gating was done to exclude GFP-negative cells, and gating for HA-positive cells were based on cells transfected with an empty vector, shown to the left.

Since CLR-antibodies can have a tendency to be cross-reactive (Miyake et al., 2013), we wanted to test the antibodies before use. None of the antibodies tested showed Mincle/Mcl cross-reactivity, but the α–mMincle Ab 4A9, and Wells' Ab to some degree, showed interspecies specificity (fig. 4.8). Values presented were obtained gating for double positive cells. Again, FcRγ was co-transfected with the CLR of interest in a 1:2 ratio. Cell plots and gating for all antibodies can be found in appendix II.

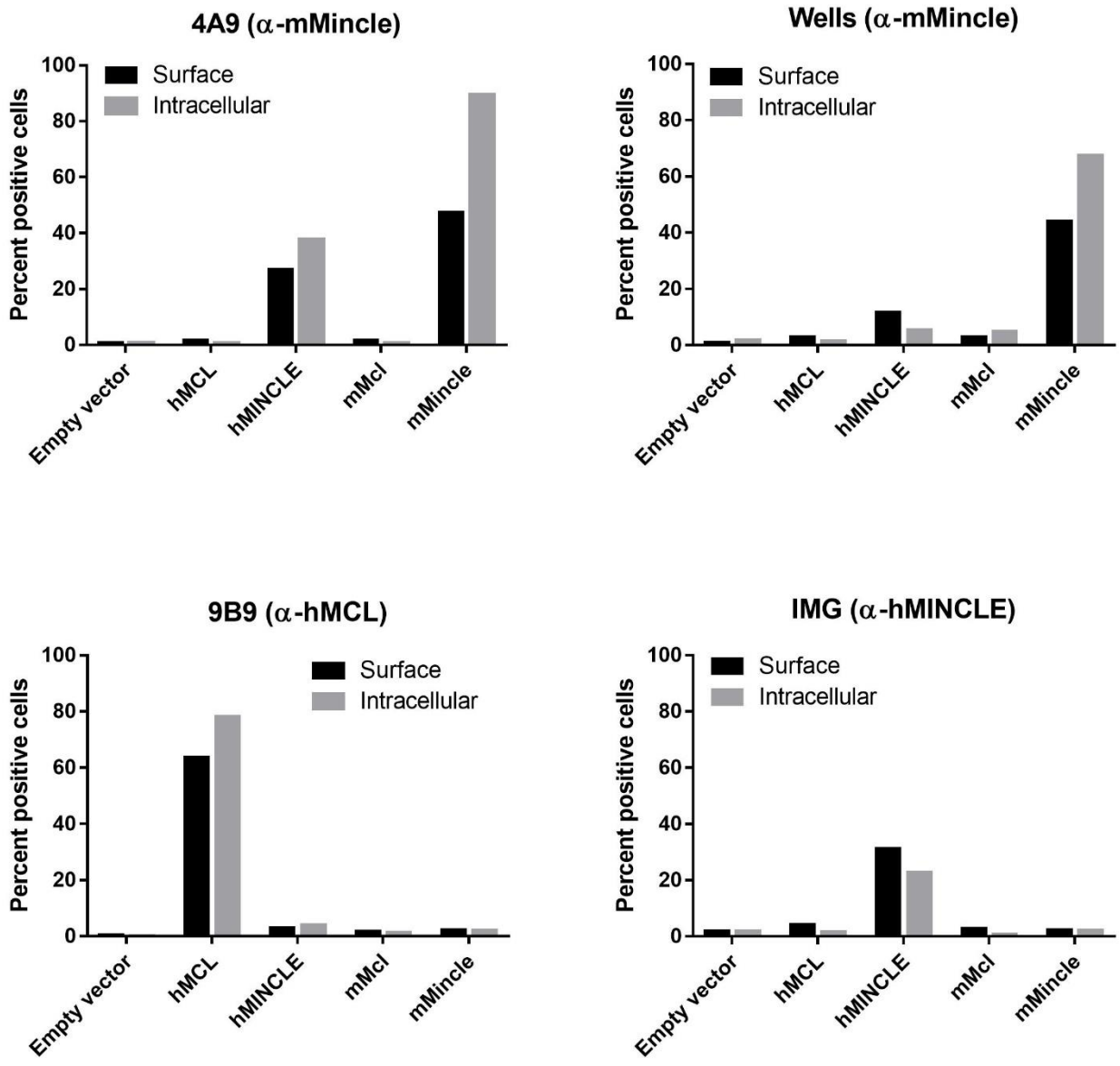

Figure 4.8 Antibody specificity test. Specificity of four different antibodies tested on over-expressing HEK293 cells transiently transfected with different constructs were measured by flow cytometry. Surface staining shown in black, intracellular staining shown in grey.

FcRγ is beneficial, but not essential for surface localization of mMincle in HEK293 cells. FcRγ has been shown to be essential for Mincle signalling (Lobato-Pascual et al., 2013; Schoenen et al., 2014; Yamasaki et al., 2008), and to increase surface expression of Mincle (Yamasaki et al., 2008). We wanted to test whether FcRγ was needed for surface expression of Mincle in over-expressing HEK293 cells. HEK293 cells were transiently transfected with only mMincle-HA or mMincle-HA together with FcRγ (1:2 ratio). Specimens were stained and measured by flow cytometry, gating for GFP and 4A9 or α–HA positives.

Data (fig. 4.9) indicates that surface expression of mMincle in over-expressing HEK293 cells is not dependent on FcRγ, but FcRγ seems to increase the surface expression. The results also imply that the 4A9 and α-HA antibody were roughly equally sensitive for use in flow cytometry.

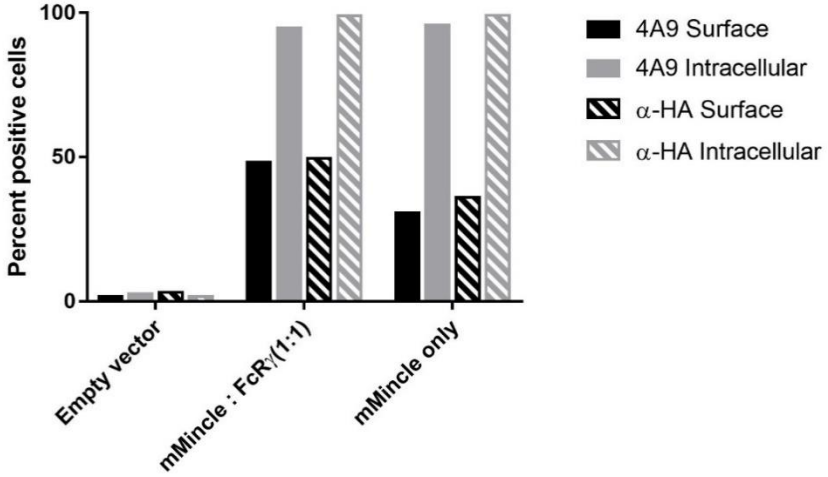

Figure 4.9 FcRγ is beneficial, but not essential for surface localization of Mincle. Expression of mMincle with and without FcRγ in transiently transfected and overexpressing HEK293 cells, measured by flow cytometry. Gating was done using cells transfected with an empty vector.

Antibody-testing using scanning confocal microscopy

Antibodies tested were found to be specific for their respective CLR in flow cytometry (fig. 4.8). The commercially available 4A9 Ab (α–mMincle) was tested for use in confocal microscopy to confirm its performance, also in this application. HEK293 cells were transiently transfected with an empty vector, murine or human Mincle or Mcl, or an HA-tagged mMincle as a positive control, together with FcRγ (1:2).

As shown in fig. 4.10, the 4A9 Ab was found to be specific for imaging of over-expressing HEK293 cells using scanning confocal microscopy, both for human and murine Mincle. In these cells, both murine and human Mincle were mainly localized to the plasma membrane and around the nucleus (fig. 4.10).

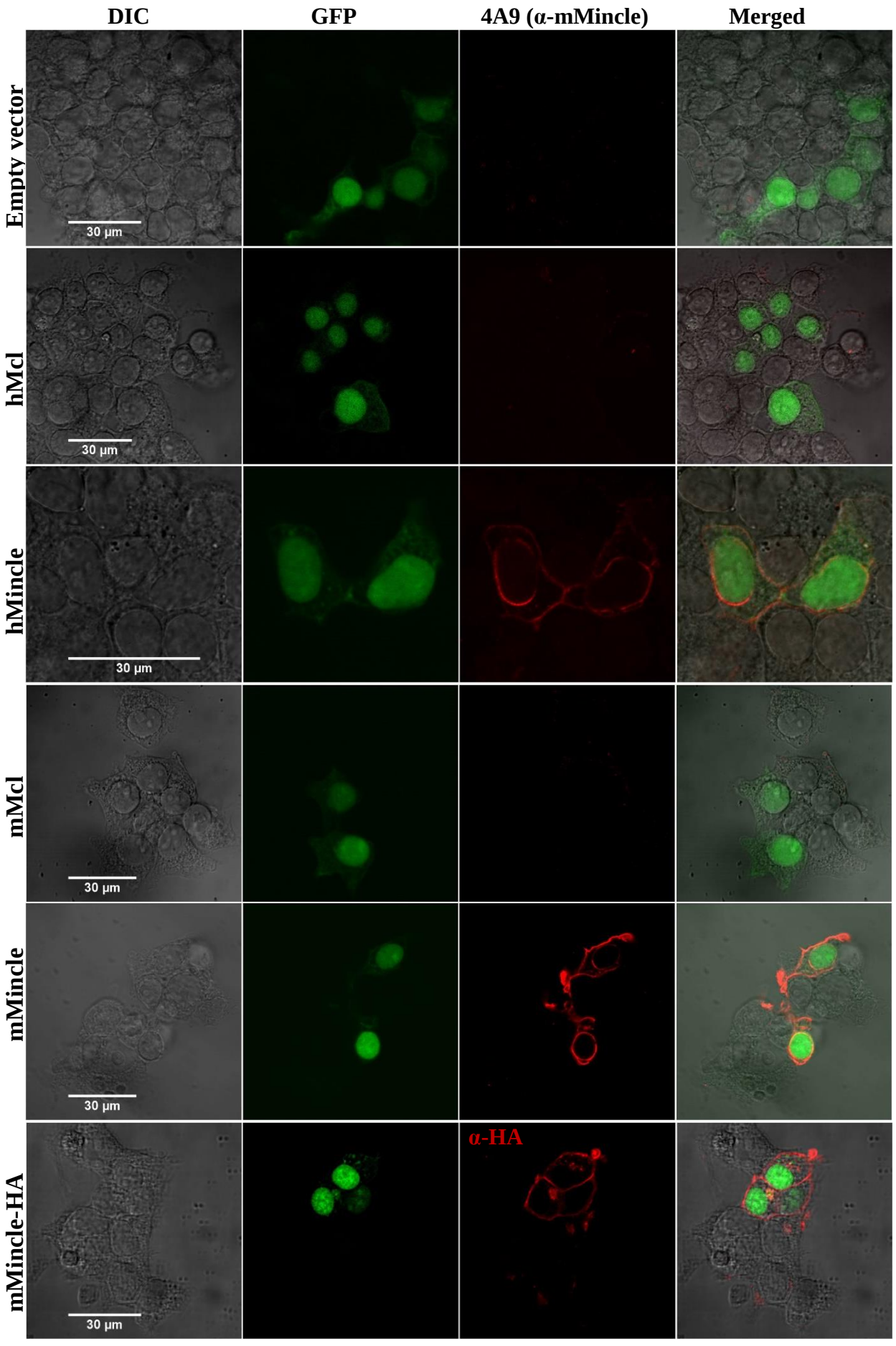
DIC
GFP
4A9 (α-mMincle)
Merged
Empty vector
hMcl
hMincle
mMcl
mMincle
mMincle-HA
30 µm
α-HA

Figure 4.10 Mincle is localized on the plasma membrane and around the nucleus in overexpressing HEK293 cells. Overexpressing HEK293 cells stained with the 4A9 Ab. All plasmids used for transfection encoded GFP. A negative control (empty vector) is shown in the top row, and the bottom row shows the positive control (mMincle-HA stained with α-HA).

4.2.2 Staining of primary WT and Mincle$^{-/-}$ BMMs

To study the localization of Mincle, different staining procedures and antibodies were tested on primary WT and Mincle$^{-/-}$ BMMs. The BMMs were primed with LPS or kept unstimulated, and specimens were studied using scanning confocal microscopy. Two different fixation- and staining procedures were tested (see section 3.6 for details): either using PFA followed by permeabilization using saponin, or methanol/acetone (1:2). For the antibodies tested, no difference was observed between the two staining procedures. In following experiments and results presented, PFA-fixation was used.

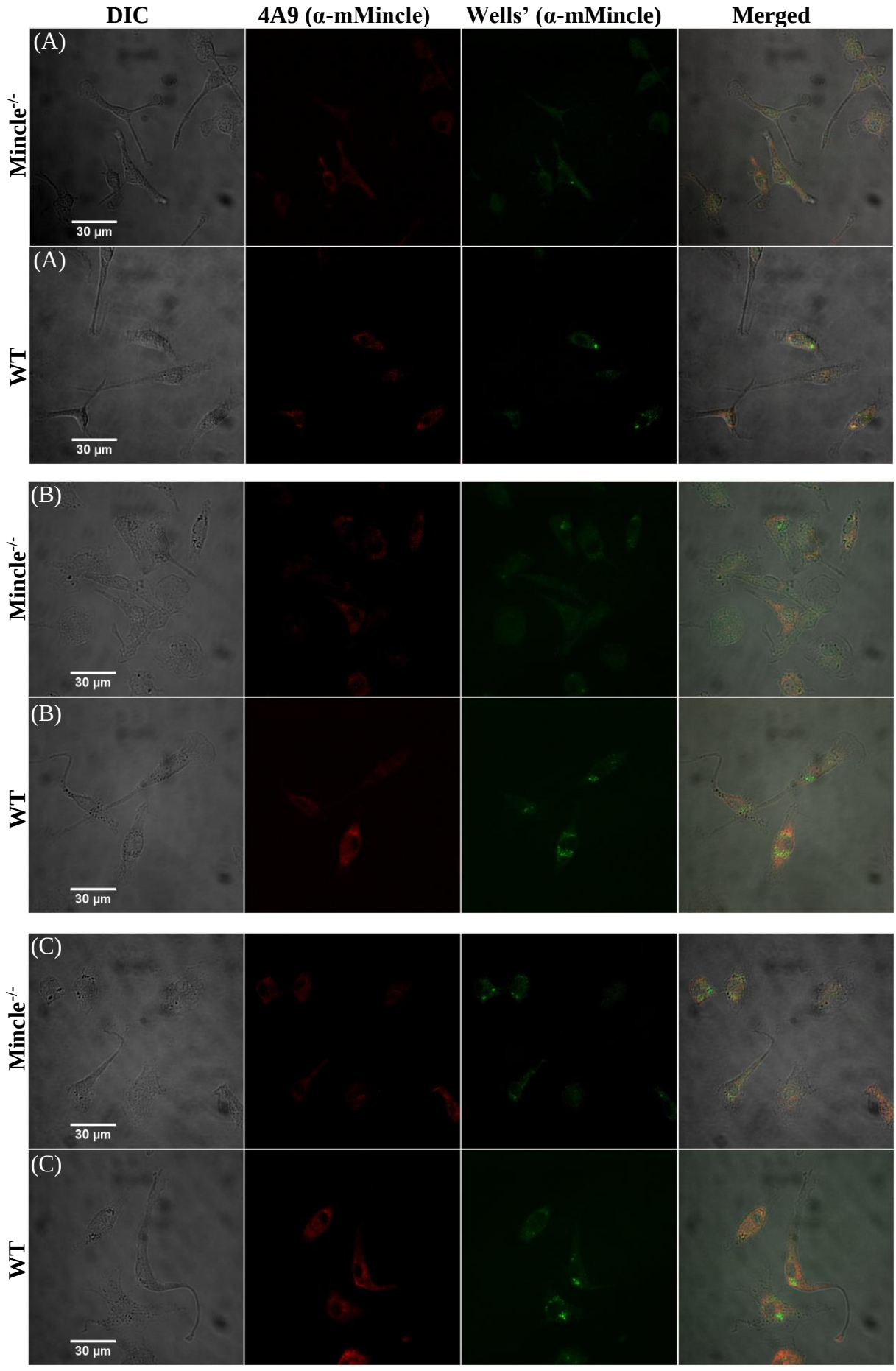
DIC
4A9 (α-mMincle)
Wells' (α-mMincle)
Merged
Mincle-/-
WT
(A)
(B)
(C)
30 µm

Figure 4.11 Comparison of stained WT and Mincle$^{-/-}$ BMMs. The figure compares fixed WT and Mincle$^{-/-}$ BMMs stained with two different α-mMincle antibodies; 4A9 (red) and Wells' Ab (green). The cells were left unstimulated (A) or stimulated with LPS overnight, either 10 ng/ml (B) or 100 ng/ml (C). All images were taken using the same settings.

When stained WT and Mincle$^{-/-}$ BMMs were compared, no visible differences were observed for the untreated specimens (fig. 4.11A) while minor differences could be observed in the LPS-treated specimens despite high background (fig. 4.11 B, C).

To further increase the signal-to-noise ratio of Mincle-stained primary cells, we decided to proceed with overexpression studies, shown in the next section (4.2.3).

4.2.3 Retroviral transduction of WT and Mincle$^{-/-}$ BMMs and BMDCs

The 4A9 Ab was found to be specific for human and murine Mincle in overexpressing HEK293 cells when tested using flow cytometry and confocal microscopy (fig. 4.8 and 4.10, respectively). In overexpressing HEK293 cells, Mincle was mainly localized to the plasma membrane and around the nucleus (fig. 4.10). Preliminary results from staining of LPS-primed primary cells (fig. 4.11 B and C) indicated that Mincle was more evenly distributed in primary cells. Increased expression levels and the possibility to introduce tags would be advantageous to obtain more conclusive data. Retroviral transduction was therefore used to establish tools for further assessment of Mincle localization in BMMs and BMDCs during infection with *M. avium*.

Retroviral transduction of WT BMMs and BMDCs

Phoenix Eco cells were transfected with the CLR of interest or an empty vector and used as packaging cells to make virus particles, and subsequent retroviral transduction of WT BMMs and BMDCs was done as a test. A working procedure was established after some optimization, results are shown in fig. 4.12 and 4.13. Before fixation and imaging, the cells were incubated with LPS (10 ng/ml) overnight to increase adherence to the glass surface.

4A9 staining is presented in fig. 4.12 – 4.15 and fig. 4.17 while an example of α-HA staining is shown in fig. 4.16.

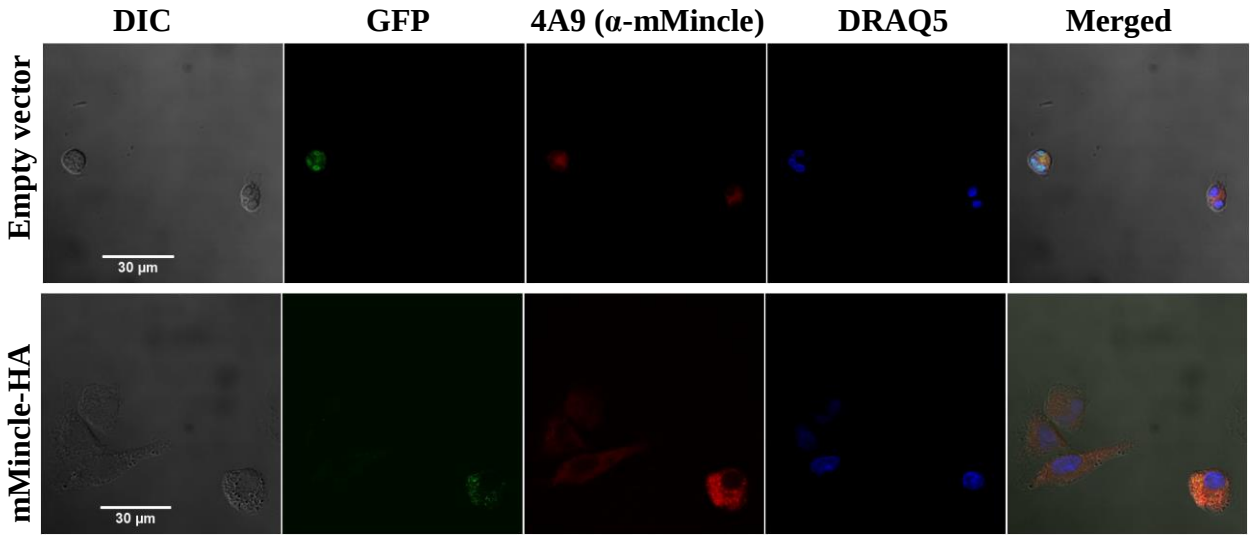

Figure 4.12 Transduced WT BMDCs. The figure shows transduced WT BMDC, fixed and stained with 4A9 (α-mMincle) and the nuclear stain DRAQ5. Both plasmids encoded GFP.

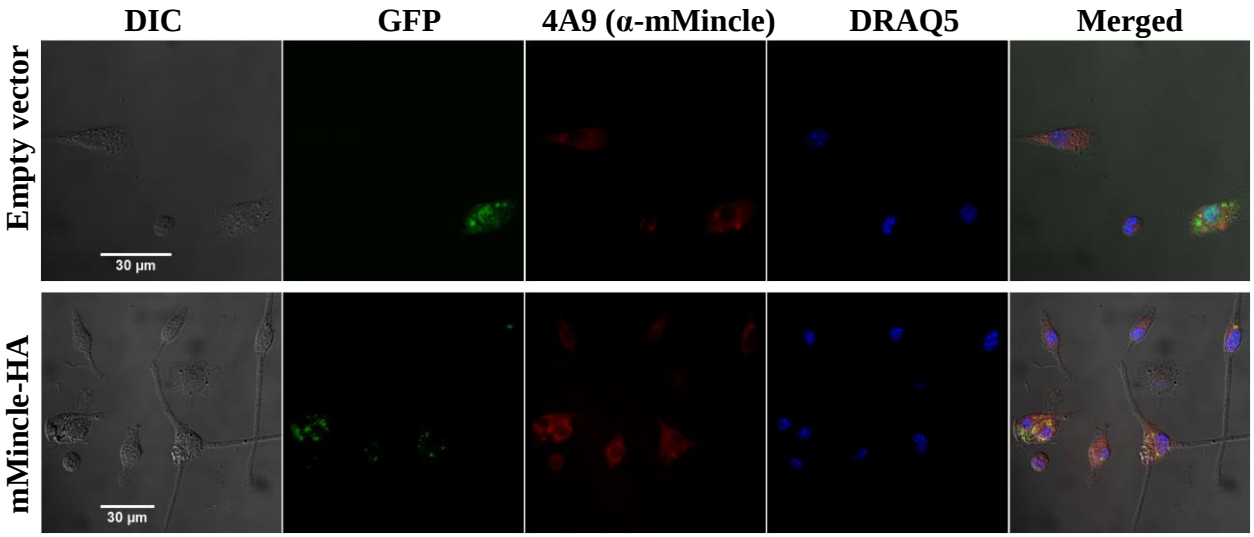

Figure 4.13 Transduced WT BMMs. The figure shows transduced WT BMMs, fixed and stained with 4A9 (α-mMincle) and the nuclear stain DRAQ5. Both plasmids encoded GFP.

Retroviral transduction of Mincle$^{-/-}$ BMMs and BMDCs

Preliminary transduction of WT BMMs and BMDCs was successful. Yet, for use in infection studies, results could be hard to interpret on WT background, and the same procedure was therefore applied to Mincle$^{-/-}$ BMMs and BMDCs. The cells were imaged using scanning confocal microscopy, results are shown in fig. 4.14 – 4.15.

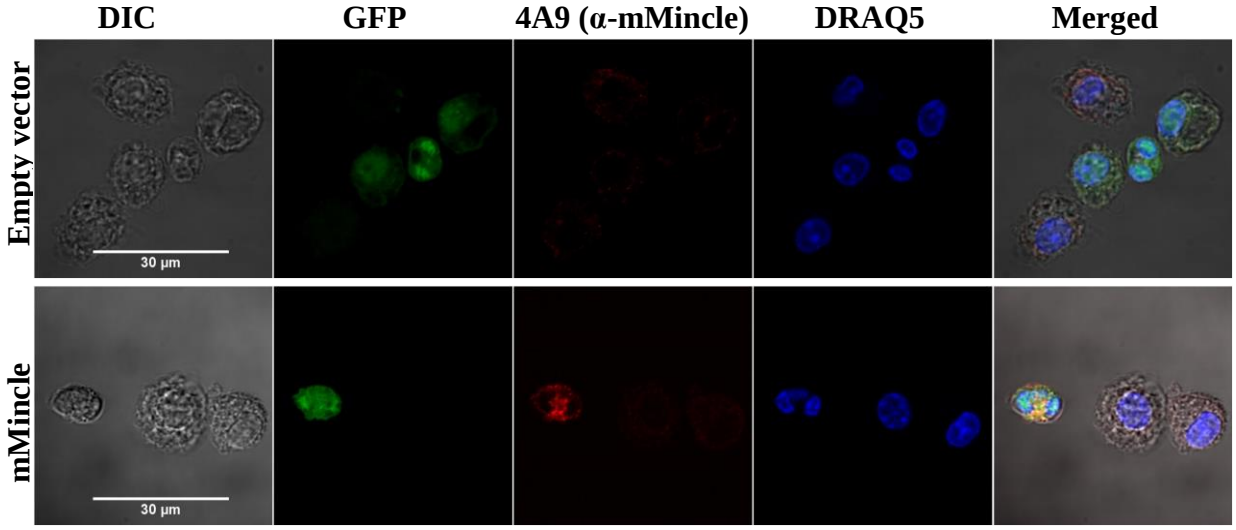

Figure 4.14 Transduced Mincle$^{-/-}$ BMDCs. The figure shows transduced Mincle$^{-/-}$ BMDCs, fixed and stained with 4A9 (α-mMincle) and the nuclear stain DRAQ5. Both plasmids encoded GFP.

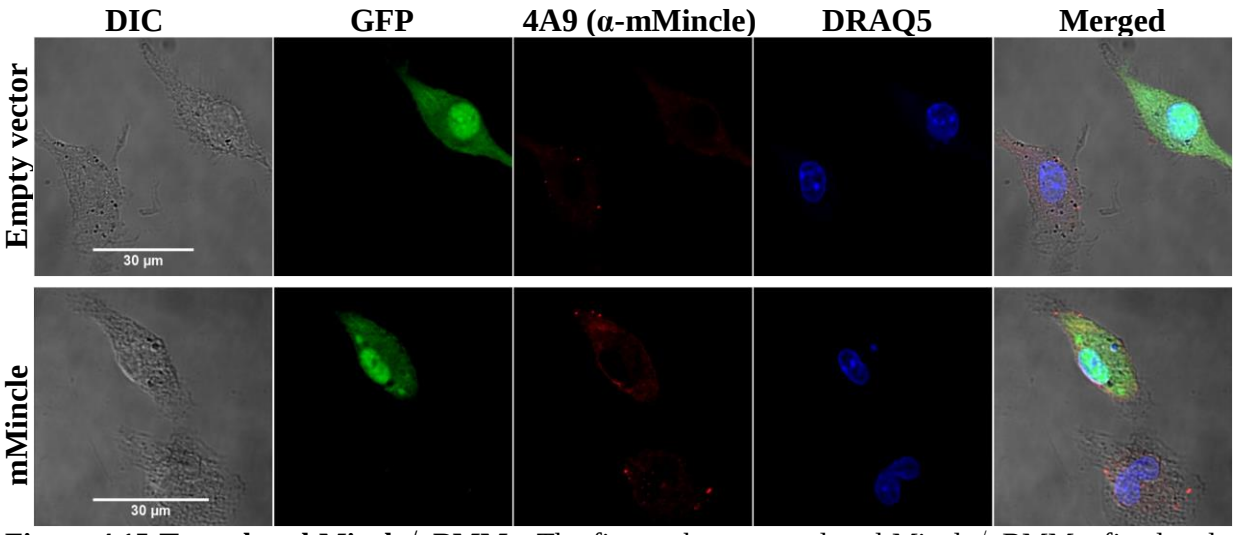

Figure 4.15 Transduced Mincle$^{-/-}$ BMMs. The figure shows transduced Mincle$^{-/-}$ BMMs, fixed and stained with 4A9 (α-mMincle) and the nuclear stain DRAQ5. Both plasmids encoded GFP.

As shown in fig. 4.12 – 4.15, we did indeed manage to establish a procedure for overexpression of Mincle in primary BMMs and BMDCs. Staining with the α-HA Ab would avoid the background observed using 4A9, also for WT cells. An example of α-HA stain is shown in fig. 4.16, implying a mostly intracellular localization for Mincle. Preliminary results from mMincle-transduced Mincle$^{-/-}$ BMMs infected with *M. avium* (MOI 5, overnight) did not indicate an increased concentration of Mincle around the phagocytosed mycobacteria (fig. 4.17).

Keeping in mind that GFP expression is not a perfect marker for successful transduction and Mincle-expression, this method can now be used for infection experiments.

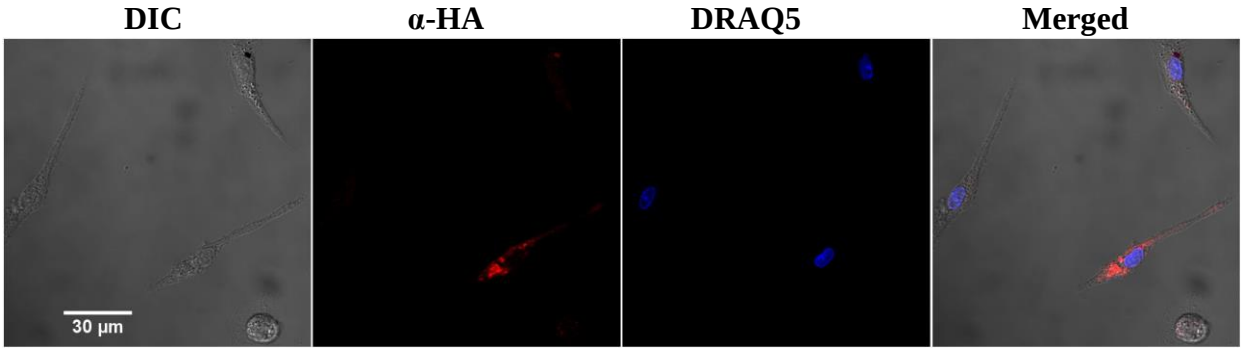

Figure 4.16 Example of HA-staining. The figure shows a transduced WT BMM, overexpressing mMincle-HA, stained with α-HA Ab and a nuclear stain (DRAQ5).

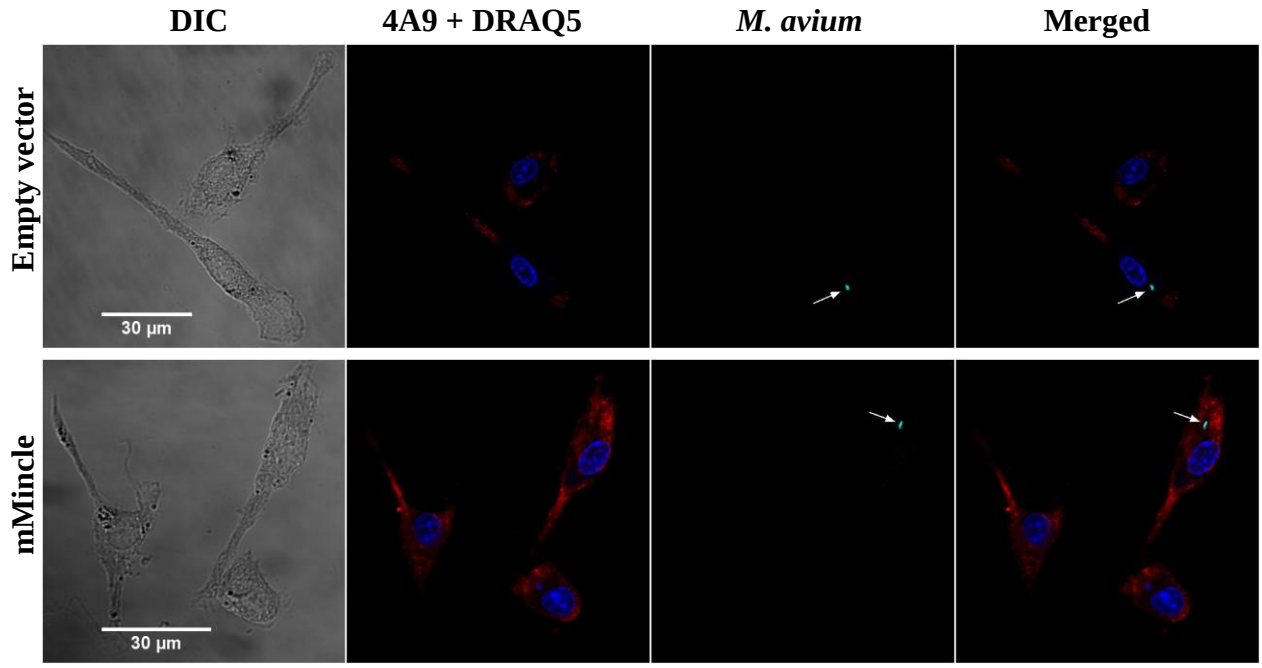

Figure 4.17 Example of transduced Mincle$^{-/-}$ BMMs infected with *M. avium*. Mincle$^{-/-}$ BMMs transduced with mMincle or empty vector were infected with CFP^{+} *M. avium* (MOI 10) and PFA-fixed after 2 hours. Cells were stained with 4A9 (α-mMincle, red) and the nuclear stain DRAQ5 (blue). White arrows indicate phagocytosed *M. avium*.

5 Discussion and conclusion

Comparative *in vitro* experiments conducted in this study suggest a non-essential role for Mincle in *M. avium* infections. WT and Mincle-deficient BMMs did not differ in their capability to phagocytose or kill *M. avium*, and no differences were observed for secreted cytokines (KC, IL-6, IP-10 or G-CSF) associated with mycobacterial infection. In this study we also established a working tool for overexpression of Mincle, with the potential of other CLRs as well, in primary BMMs and BMDCs that can now be used for infection experiments.

Mincle and mycobacteria

Mincle has previously been found not to be essential for controlling *M. tuberculosis* (Mtb, strain H37Rv) infection in mice (Heitmann et al., 2012). Controversially, Mincle was found to be an important component of the innate immune response to *M. bovis* BCG (Behler et al., 2012; Schoenen et al., 2010). These somewhat contradictory findings, combined with the widespread occurrence of MAC infections made it interesting to test whether the absence of Mincle influenced BMMs capability to phagocytose and kill *M. avium*.

Examination of phagocytosis and killing of *M. avium* by scanning confocal microscopy (fig. 4.2B) and plating of lysate and counting of colonies (fig. 4.3), backed up the luciferase assay as a method for measuring these events. Nonetheless, no differences between WT and Mincle$^{-/-}$ BMMs in their ability to phagocytose or kill *M. avium* in early time points ($\leq$ 5 days) were indicated in this *in vitro* study, as shown in fig. 4.2 – 4.4.

This implicated non-essential role for Mincle during *M. avium* infection thereby supports previous, more comprehensive studies of Mtb infection in mice (Heitmann et al., 2012). Lee et al. on the other hand, showed that Mincle-deficient mice had higher inflammation levels (TNF, IFN-γ, IL-6) and mycobacterial loads in the lungs compared to WT mice after infection with Mtb Erdman (Lee et al., 2012). Higher bacterial load, but lower levels of inflammatory cytokines (TNF, IFN-γ, IL-1) were observed in spleens and splenic macrophages and DC of Mincle-deficient mice infected with BCG (Behler et al., 2015; Behler et al., 2012). That said, the differences observed by Lee et al. and Behler et al. manifested >7 days post infection *in vivo*, and comparing their findings with this study, both regarding phagocytosis and killing might be erroneous.

In this study, measured G-CSF, IL-6, KC and IP-10 indicated no difference between Mincle$^{-/-}$ and WT BMMs in response to *M. avium* infection, as shown in fig. 4.5.

Other studies conducted using *M. bovis* BCG have shown that Mincle-deficient BMMs have defects in the response to BCG compared to WT, demonstrated by impaired production of G-CSF and IL-6 (Schoenen et al., 2010). Alveolar Mincle$^{-/-}$ macrophages showed lower levels of TNF, MIP-2 and KC compared to WT (Behler et al., 2012). An impaired production of G-CSF by Mincle$^{-/-}$ BMMs in response to BCG and Mtb was also observed by Heitmann et al., but the levels of TNF were comparable to WT (Heitmann et al., 2012). Ishikawa et al. observed no difference in TNF secretion, and only partially impaired MIP-2 secretion by Mincle$^{-/-}$ BMMs infected with Mtb compared to WT (Ishikawa et al., 2009). Wevers et al. demonstrated that human Mincle has a suppressive role in antifungal defence by inducing degradation of interferon regulatory factor 1 and hence reduced IL-12 secretion, leading to impaired T_h1 responses (Wevers et al., 2014). This can possibly explain why WT mouse BMMs did not secrete any IL-12 of significance when exposed to *M. avium* (Signe Åsberg, unpublished results). An anti-inflammatory role of Mincle was also demonstrated by Patin et al., as Mincle-deficient BMMs exposed to TDM or BCG secreted lower levels of IL-10 (Patin et al., 2016). Together, these somewhat dissonant results can possibly be attributed to different mycobacterial strains used, total mycobacterial load, different subtypes of macrophages or route of mycobacterial infection, in addition to other differences e.g. in cultivation procedures.

Cytokines mentioned above, associated with Mincle or mycobacterial infection are mostly neutrophil-recruiting chemokines (Owen et al., 2013). Lee et al. focused on neutrophils in their study of Mincle-deficient mice and showed that recruitment of neutrophils to TDM-coated beads injected subcutaneously was dependent on Mincle expression (Lee et al., 2012). Recently, Lee et al. showed that Mincle, in addition to influencing cytokine secretion, is the key switch for the transition from cytokine expression to high nitric oxide (NO) production and later inflammation resolution in macrophages (Lee et al., 2016).

Nonetheless, differences observed between WT and Mincle- or other CLR-deficient mice show mild phenotypes compared to mice deficient in downstream signalling proteins like CARD9 (Dorhoi et al., 2010). This implicates a form of redundancy, as observed for different TLRs (Lindsay et al., 2010). When exposed to whole mycobacteria, PAMPs other than TDM are recognized by other PRRs expressed by innate immune cells (e.g. TLR 2 (Heldwein et al.,

2003)) and likely compensates for the absence of Mincle. The mild phenotypes observed for single-CLR-deficient mice raise the question if individual CLRs might not be essential, but together may contribute to shape the immune response through crosstalk with other PRRs, already addressed in several previous publications (Geijtenbeek and Gringhuis, 2009; Kerscher et al., 2016a; Kerscher et al., 2013; Lang, 2013).

Where is Mincle?

A better understanding of the different CLRs' impact and contribution in innate immune cells is of interest, because it might have functional implications. Clarifying the potential translocation of Mincle, e.g. to the phagosome and/or lysosome can indicate if signalling from Mincle in subcellular compartments can take place and whether the receptor might be recycled or not. The localization of Mincle, and where and when signalling takes place is still not fully elucidated. Preliminary results from this study indicated outspread localization of Mincle in overexpressing BMMs and BMDCs (fig. 4.12-17).

Mincle has previously been shown to be on the surface, localized to the phagocytic cup (Wells et al., 2008), indicating a role of Mincle in early phagosomes. Proteome studies have shown that Mincle is present in phagosomes from BMMs, although in low levels (Guo et al., 2015). At the same time, structural analysis of human and bovine Mincle suggests that it loses its binding activity at endosomal pH, making phagolysosomal Mincle-ligand-interaction less likely (Furukawa et al., 2013; Jegouzo et al., 2014). Given that mycobacteria and their cord factor can inhibit phagosomal maturation (Indrigo et al., 2003), these findings may not necessarily be contradictory.

Surface localization of murine Mincle has been shown in several studies, and recent studies have highlighted the importance of Mcl for surface expression of Mincle (Kerscher et al., 2016b; Lobato-Pascual et al., 2013; Miyake et al., 2015). Surface-localization also for human Mincle was implicated by Ostrop et al., albeit both Mincle and Mcl were shown to be mostly intracellular under resting conditions (Ostrop et al., 2015). Expression and surface localization of Mincle and Mcl have been shown to be interdependently coregulated during infection and inflammation (Kerscher et al., 2016b; Miyake et al., 2015). In addition to this mutual enhancement of surface expression of Mincle and Mcl, the surface expression of both receptors were found to be upregulated by MyD88-dependent signalling (Kerscher et al., 2016a).

Both Mincle and Mcl have been shown to be dependent upon FcRγ for signalling (Miyake et al., 2013; Yamasaki et al., 2008), implying a similar function. Mcl has previously been shown to be a phagocytic receptor (Arce et al., 2004; Graham et al., 2012; Lobato-Pascual et al., 2013). Immunoprecipitation of Mcl showed co-precipitation of both Dectin-2 (Zhu et al., 2013) and Mincle (Lobato-Pascual et al., 2013; Miyake et al., 2015), indicating a physical interaction. This led Zhu et al. to suggest that Mcl and Dectin-2 forms a functional heterodimer, as did Lobato-Pascual et al. for Mcl and Mincle. However, Mincle was not co-precipitated together with Mcl when human versions of the receptors were used (Zhao et al., 2014), indicating a functional difference between murine and human Mincle/Mcl.

FcRγ has been shown to be essential for Mincle signalling (Yamasaki et al., 2008), assumed to be required for surface expression of Mincle (Kerscher et al., 2016b), and shown not to be required for surface expression of Mincle in transfected HEK293 cells (Matsumoto et al., 1999). Yamasaki et al. showed that surface expression of Mincle was higher in WT BMMs than in FcRγ-deficient BMMs (Yamasaki et al., 2008). In our study, HEK293 cells transfected with mMincle-HA ± FcRγ (fig. 4.9) indicated that FcRγ was not essential for, but increased the surface expression of Mincle, in line with both Yamasaki et al. and Matsumoto et al.

Future perspectives

The tools established in this study enable overexpression of different CLRs through retroviral transduction of primary BMMs and BMDCs. Although BMMs and BMDCs are considered notoriously hard to transfect, a combination of electroporation and reagents (Nucleofection™, Amaxa/Lonza) have had some success (Aluigi et al., 2006; Gresch and Altrogge, 2012) and might serve as an alternative to retroviral transduction.

HA-tagged Mincle was functionally comparable to the untagged version in response to TDB and TDM (Ostrop, 2015). Whether the HA-tag might alter the localization of Mincle in primary BMMs or BMDCs would be natural to test for before using HA-tagged Mincle in future localization- and infection studies. Preliminary results from HEK293 cells did not indicate a difference in localization between untagged and HA-tagged Mincle (fig 4.10).

Where Mincle and Mcl are localized at different time points in mycobacterial infection is of great interest, because may have functional implications. Results from BMMs infected with *M. avium* (fig. 4.17) are only preliminary, but at this time point, an increased concentration of

Mincle around the phagocytosed mycobacteria was not indicated. One possible explanation is of course that Mincle is not there, another is that if Mincle is bound to the mycobacteria, the 4A9 binding epitope might be occupied or not accessible. HA-staining might circumvent that possibility, although steric hindrance may still be an issue, as the HA-tag is linked to the extracellular C-terminus of Mincle. Timing could also be an issue, and imaging at different time points could possibly reveal new information as well.

Antibodies specific for murine Mcl (Kerscher et al., 2016b) are now available in our lab, opening up for the possibility to further elucidate the suggested heterodimerization of Mincle and Mcl. The role of Mcl and/or FcRγ for the localization of Mincle in primary cells can also be further investigated by overexpressing combinations of Mincle, Mcl and FcRγ. Co-staining of Mincle and FcRγ could help to resolve several questions, such as: where do Mincle and FcRγ meet; how is trafficking regulated; and what is the role of FcRγ for Mincle surface expression? Another possibility in this overexpressing model is to compare the localization of Mincle and/or Mcl after stimulation with structurally different ligands, e.g. TDB-coated beads, brartemicin, whole mycobacteria, cholesterol crystals or SAP130. Maybe there is a discrepancy between soluble and particulate ligands, as described for Dectin-1 (Goodridge et al., 2011)?

Finally, co-localization studies of Mincle/Mcl and proteins of known localization in infections with different mycobacteria could reveal new information. Co-staining combined with time-course imaging could for instance make it possible to determine if Mincle goes to the phagosome, to late endosomes (e.g. EEA1 stain) and lysosome (e.g. LAMP1 stain).

Taken together, results from this study indicated a non-essential role for Mincle in *M. avium*-infected BMMs during the first five days of infection. To further elucidate the localization, and thereby the potential role of Mincle during mycobacterial infection, anti-Mincle antibodies have been tested for use in confocal microscopy. A method for overexpression of CLRs in primary BMM/DCs has also been tested and established, which can be applied in future experiments.

References

Achkar, J.M., J. Chan, and A. Casadevall. 2015. Role of B cells and antibodies in acquired immunity against Mycobacterium tuberculosis. *Cold Spring Harb. Perspect. Med.* 5:a018432.

Aderem, A., and D.M. Underhill. 1999. Mechanisms of phagocytosis in macrophages. *Annu Rev Immunol*. 17:593-623.

Ahsan, M.J. 2015. Recent advances in the development of vaccines for tuberculosis. *Therapeutic Advances in Vaccines*. 3:66-75.

Aluigi, M., M. Fogli, A. Curti, A. Isidori, E. Gruppioni, C. Chiodoni, M.P. Colombo, P. Versura, A. D'Errico-Grigioni, E. Ferri, M. Baccarani, and R.M. Lemoli. 2006. Nucleofection is an efficient nonviral transfection technique for human bone marrow-derived mesenchymal stem cells. *Stem Cells*. 24:454-461.

Arce, I., L. Martinez-Munoz, P. Roda-Navarro, and E. Fernandez-Ruiz. 2004. The human C-type lectin CLECSF8 is a novel monocyte/macrophage endocytic receptor. *Eur. J. Immunol.* 34:210-220.

Archuleta, R.J., P. Yvonne Hoppes, and T.P. Primm. 2005. Mycobacterium avium enters a state of metabolic dormancy in response to starvation. *Tuberculosis (Edinburgh, Scotland)*. 85:147-158.

Behler, F., R. Maus, J. Bohling, S. Knippenberg, G. Kirchhof, M. Nagata, D. Jonigk, N. Izykowski, L. Magel, T. Welte, S. Yamasaki, and U.A. Maus. 2015. Macrophage-inducible C-type lectin Mincle-expressing dendritic cells contribute to control of splenic Mycobacterium bovis BCG infection in mice. *Infect. Immun.* 83:184-196.

Behler, F., K. Steinwede, L. Balboa, B. Ueberberg, R. Maus, G. Kirchhof, S. Yamasaki, T. Welte, and U.A. Maus. 2012. Role of Mincle in alveolar macrophage-dependent innate immunity against mycobacterial infections in mice. *J Immunol*. 189:3121-3129.

Behr, M.A. 2002. BCG — different strains, different vaccines? *The Lancet Infectious Diseases*. 2:86-92.

Bekierkunst, A., I.S. Levij, E. Yarkoni, E. Vilkas, A. Adam, and E. Lederer. 1969. Granuloma formation induced in mice by chemically defined mycobacterial fractions. *J. Bacteriol.* 100:95-102.

Ben Salah, I., T. Adekambi, D. Raoult, and M. Drancourt. 2008. rpoB sequence-based identification of Mycobacterium avium complex species. *Microbiology*. 154:3715-3723.

Boon, C., and T. Dick. 2012. How Mycobacterium tuberculosis goes to sleep: the dormancy survival regulator DosR a decade later. *Future Microbiol.* 7:513-518.

Brode, S.K., C.L. Daley, and T.K. Marras. 2014. The epidemiologic relationship between tuberculosis and non-tuberculous mycobacterial disease: a systematic review. *The International Journal of Tuberculosis and Lung Disease*. 18:1370-1377.

Cassidy, P.M., K. Hedberg, A. Saulson, E. McNelly, and K.L. Winthrop. 2009. Nontuberculous Mycobacterial Disease Prevalence and Risk Factors: A Changing Epidemiology. *Clin. Infect. Dis.* 49:e124-e129.

Cayer, M.-P., M. Veillette, P. Pageau, R. Hamelin, M.-J. Bergeron, A. Mériaux, Y. Cormier, and C. Duchaine. 2007. Identification of mycobacteria in peat moss processing plants: application of molecular biology approaches. *Can. J. Microbiol.* 53:92-99.

Costello, A.M., A. Kumar, V. Narayan, M.S. Akbar, S. Ahmed, C. Abou-Zeid, G.A. Rook, J. Stanford, and C. Moreno. 1992. Does antibody to mycobacterial antigens, including lipoarabinomannan, limit dissemination in childhood tuberculosis? *Trans. R. Soc. Trop. Med. Hyg.* 86:686-692.

Covert, T.C., M.R. Rodgers, A.L. Reyes, and G.N. Stelma. 1999. Occurrence of nontuberculous mycobacteria in environmental samples. *Appl. Environ. Microbiol.* 65:2492-2496.

Daley, C.L., and D.E. Griffith. 2010. Pulmonary non-tuberculous mycobacterial infections. *Int. J. Tuberc. Lung Dis.* 14:665-671.

Dambuza, I.M., and G.D. Brown. 2015. C-type lectins in immunity: recent developments. *Curr. Opin. Immunol.* 32:21-27.

Darouiche, R.O., A. Koff, T. Rosen, T.V. Darnule, M.D. Lidsky, and F.A. El-Zaatari. 1996. Recurrent disseminated infection with Mycobacterium avium complex identified in tissues by molecular analysis. *Clin. Infect. Dis.* 22:714-715.

Dawson, D. 1971. Potential pathogens among strains of mycobacteria isolated from house-dusts. *The Medical Journal of Australia*. 1:679.

De Groote, M.A., N.R. Pace, K. Fulton, and J.O. Falkinham. 2006. Relationships between Mycobacterium isolates from patients with pulmonary mycobacterial infection and potting soils. *Appl. Environ. Microbiol.* 72:7602-7606.

Dorhoi, A., C. Desel, V. Yeremeev, L. Pradl, V. Brinkmann, H.-J. Mollenkopf, K. Hanke, O. Gross, J. Ruland, and S.H.E. Kaufmann. 2010. The adaptor molecule CARD9 is essential for tuberculosis control. *The Journal of Experimental Medicine*. 207:777-792.

Dorman, S.E., C. Picard, D. Lammas, K. Heyne, J.T. van Dissel, R. Baretto, S.D. Rosenzweig, M. Newport, M. Levin, J. Roesler, D. Kumararatne, J.L. Casanova, and S.M. Holland. 2004. Clinical features of dominant and recessive interferon gamma receptor 1 deficiencies. *Lancet*. 364:2113-2121.

Egelund, E.F., K.P. Fennelly, and C.A. Peloquin. 2015. Medications and monitoring in nontuberculous mycobacteria infections. *Clin. Chest Med.* 36:55-66.

Ehrt, S., and D. Schnappinger. 2009. Mycobacterial survival strategies in the phagosome: defence against host stresses. *Cell. Microbiol.* 11:1170-1178.

Falkinham III, J., M. Iseman, P. Haas, and D. Soolingen. 2008. Mycobacterium avium in a shower linked to pulmonary disease. *Journal of water and health*. 6:209-213.

Falkinham, I.J.O. 2009. Surrounded by mycobacteria: nontuberculous mycobacteria in the human environment. *J. Appl. Microbiol.* 107:356-367.

Farhi, D.C., U.G. Mason, 3rd, and C.R. Horsburgh, Jr. 1986. Pathologic findings in disseminated Mycobacterium avium-intracellulare infection. A report of 11 cases. *Am. J. Clin. Pathol.* 85:67-72.

Field, S.K., D. Fisher, and R.L. Cowie. 2004. Mycobacterium avium complex pulmonary disease in patients without HIV infection. *CHEST Journal*. 126:566-581.

Fischer, K., D. Chatterjee, J. Torrelles, P.J. Brennan, S.H. Kaufmann, and U.E. Schaible. 2001. Mycobacterial lysocardiolipin is exported from phagosomes upon cleavage of cardiolipin by a macrophage-derived lysosomal phospholipase A2. *J Immunol*. 167:2187-2192.

Flynn, J.L., and J. Chan. 2001. Tuberculosis: latency and reactivation. *Infect. Immun.* 69:4195-4201.

Furukawa, A., J. Kamishikiryo, D. Mori, K. Toyonaga, Y. Okabe, A. Toji, R. Kanda, Y. Miyake, T. Ose, S. Yamasaki, and K. Maenaka. 2013. Structural analysis for glycolipid recognition by the C-type lectins Mincle and MCL. *Proc. Natl. Acad. Sci. U. S. A.* 110:17438-17443.

Geijtenbeek, T.B., and S.I. Gringhuis. 2009. Signalling through C-type lectin receptors: shaping immune responses. *Nat. Rev. Immunol.* 9:465-479.

Geisel, R.E., K. Sakamoto, D.G. Russell, and E.R. Rhoades. 2005. In vivo activity of released cell wall lipids of Mycobacterium bovis bacillus Calmette-Guerin is due principally to trehalose mycolates. *J Immunol*. 174:5007-5015.

Gengenbacher, M., and S.H. Kaufmann. 2012. Mycobacterium tuberculosis: success through dormancy. *FEMS Microbiol. Rev.* 36:514-532.

Goodridge, H.S., C.N. Reyes, C.A. Becker, T.R. Katsumoto, J. Ma, A.J. Wolf, N. Bose, A.S. Chan, A.S. Magee, M.E. Danielson, A. Weiss, J.P. Vasilakos, and D.M. Underhill. 2011. Activation of the innate immune receptor Dectin-1 upon formation of a 'phagocytic synapse'. *Nature*. 472:471-475.

Graham, L.M., V. Gupta, G. Schafer, D.M. Reid, M. Kimberg, K.M. Dennehy, W.G. Hornsell, R. Guler, M.A. Campanero-Rhodes, A.S. Palma, T. Feizi, S.K. Kim, P. Sobieszczuk, J.A. Willment, and G.D. Brown. 2012. The C-type lectin receptor CLECSF8 (CLEC4D) is expressed by myeloid cells and triggers cellular activation through Syk kinase. *J Biol Chem*. 287:25964-25974.

Gresch, O., and L. Altrogge. 2012. Transfection of difficult-to-transfect primary mammalian cells. *Methods Mol. Biol.* 801:65-74.

Gruenberg, J., and H. Stenmark. 2004. The biogenesis of multivesicular endosomes. *Nature reviews Molecular cell biology*. 5:317-323.

Guo, M., A. Härtlova, B.D. Dill, A.R. Prescott, M. Gierliński, and M. Trost. 2015. High-resolution quantitative proteome analysis reveals substantial differences between phagosomes of RAW 264.7 and bone marrow derived macrophages. *PROTEOMICS*. 15:3169-3174.

Gutierrez, M.G., S.S. Master, S.B. Singh, G.A. Taylor, M.I. Colombo, and V. Deretic. 2004. Autophagy is a defense mechanism inhibiting BCG and Mycobacterium tuberculosis survival in infected macrophages. *Cell*. 119:753-766.

Halstrom, S., P. Price, and R. Thomson. 2015. Review: Environmental mycobacteria as a cause of human infection. *International Journal of Mycobacteriology*. 4:81-91.

Haug, C.J., P. Aukrust, E. Lien, F. Muller, T. Espevik, and S.S. Froland. 1996. Disseminated Mycobacterium avium complex infection in AIDS: immunopathogenic significance of an

activated tumor necrosis factor system and depressed serum levels of 1,25 dihydroxyvitamin D. *J. Infect. Dis.* 173:259-262.

Heitmann, L., H. Schoenen, S. Ehlers, R. Lang, and C. Hölscher. 2012. Mincle is not essential for controlling Mycobacterium tuberculosis infection. *Immunobiology*. 218:506-516.

Heldwein, K.A., M.D. Liang, T.K. Andresen, K.E. Thomas, A.M. Marty, N. Cuesta, S.N. Vogel, and M.J. Fenton. 2003. TLR2 and TLR4 serve distinct roles in the host immune response against Mycobacterium bovis BCG. *J. Leukoc. Biol.* 74:277-286.

Henkle, E., and K.L. Winthrop. 2015. Nontuberculous mycobacteria infections in immunosuppressed hosts. *Clin. Chest Med.* 36:91-99.

Hermansen, T.S., V.Ø. Thomsen, T. Lillebaek, and P. Ravn. 2014. Non-Tuberculous Mycobacteria and the Performance of Interferon Gamma Release Assays in Denmark. *PLoS ONE*. 9:e93986.

Hestvik, A.L.K., Z. Hmama, and Y. Av-Gay. 2005. Mycobacterial manipulation of the host cell. *FEMS Microbiol. Rev.* 29:1041-1050.

Huynh, K.K., and S. Grinstein. 2007. Regulation of vacuolar pH and its modulation by some microbial species. *Microbiol. Mol. Biol. Rev.* 71:452-462.

Iivanainen, E.K., P.J. Martikainen, M.L. Räisänen, and M.-L. Katila. 1997. Mycobacteria in boreal coniferous forest soils. *FEMS Microbiol. Ecol.* 23:325-332.

Indrigo, J., R.L. Hunter, Jr., and J.K. Actor. 2003. Cord factor trehalose 6,6'-dimycolate (TDM) mediates trafficking events during mycobacterial infection of murine macrophages. *Microbiology*. 149:2049-2059.

Ishikawa, E., T. Ishikawa, Y.S. Morita, K. Toyonaga, H. Yamada, O. Takeuchi, T. Kinoshita, S. Akira, Y. Yoshikai, and S. Yamasaki. 2009. Direct recognition of the mycobacterial glycolipid, trehalose dimycolate, by C-type lectin Mincle. *J. Exp. Med.* 206:2879-2888.

Ishikawa, T., F. Itoh, S. Yoshida, S. Saijo, T. Matsuzawa, T. Gonoi, T. Saito, Y. Okawa, N. Shibata, T. Miyamoto, and S. Yamasaki. 2013. Identification of distinct ligands for the C-type lectin receptors Mincle and Dectin-2 in the pathogenic fungus Malassezia. *Cell Host Microbe*. 13:477-488.

Jegouzo, S.A., E.C. Harding, O. Acton, M.J. Rex, A.J. Fadden, M.E. Taylor, and K. Drickamer. 2014. Defining the conformation of human mincle that interacts with mycobacterial trehalose dimycolate. *Glycobiology*. 24:1291-1300.

Johnson, M.M., and J.A. Odell. 2014. Nontuberculous mycobacterial pulmonary infections. *J. Thorac. Dis.* 6:210-220.

Kaufmann, S.H.E., T.G. Evans, and W.A. Hanekom. 2015. Tuberculosis vaccines: Time for a global strategy. *Sci. Transl. Med.* 7:276fs278-276fs278.

Kawata, K., P. Illarionov, T. Kenny, W. Zhang, M. Tsuda, Y. Ando, P. Leung, A.A. Ansari, and M.E. Gershwin. 2012. Mincle and human B cell function. *J. Autoimmun.* 39:315-322.

Kazda, J., and I. Pavlik. 2009. Obligate Pathogenic Mycobacteria. *In* The Ecology of Mycobacteria: Impact on Animal's and Human's Health. Springer Netherlands. 13-19.

Kerscher, B., I.M. Dambuza, M. Christofi, D.M. Reid, S. Yamasaki, J.A. Willment, and G.D. Brown. 2016a. Signalling through MyD88 drives surface expression of the mycobacterial receptors MCL (Clecsf8, Clec4d) and Mincle (Clec4e) following microbial stimulation. *Microbes and infection / Institut Pasteur*.

Kerscher, B., J.A. Willment, and G.D. Brown. 2013. The Dectin-2 family of C-type lectin-like receptors: an update. *Int. Immunol.* 25:271-277.

Kerscher, B., G.J. Wilson, D.M. Reid, D. Mori, J.A. Taylor, G.S. Besra, S. Yamasaki, J.A. Willment, and G.D. Brown. 2016b. Mycobacterial receptor, Clec4d (CLECSF8, MCL), is coregulated with Mincle and upregulated on mouse myeloid cells following microbial challenge. *Eur. J. Immunol.* 46:381-389.

Killick, K.E., C. Ní Cheallaigh, C. O'Farrelly, K. Hokamp, D.E. MacHugh, and J. Harris. 2013. Receptor-mediated recognition of mycobacterial pathogens. *Cell. Microbiol.* 15:1484-1495.

Kingeter, L.M., and X. Lin. 2012. C-type lectin receptor-induced NF-[kgr]B activation in innate immune and inflammatory responses. *Cell. Mol. Immunol.* 9:105-112.

Kiyotake, R., M. Oh-Hora, E. Ishikawa, T. Miyamoto, T. Ishibashi, and S. Yamasaki. 2015. Human Mincle Binds to Cholesterol Crystals and Triggers Innate Immune Responses. *J Biol Chem*. 290:25322-25332.

Lang, R. 2013. Recognition of the mycobacterial cord factor by Mincle: relevance for granuloma formation and resistance to tuberculosis. *Front. Immunol.* 4.

Lee, W.B., J.S. Kang, W.Y. Choi, Q. Zhang, C.H. Kim, U.Y. Choi, J. Kim-Ha, and Y.J. Kim. 2016. Mincle-mediated translational regulation is required for strong nitric oxide production and inflammation resolution. *Nature communications*. 7:11322.

Lee, W.B., J.S. Kang, J.J. Yan, M.S. Lee, B.Y. Jeon, S.N. Cho, and Y.J. Kim. 2012. Neutrophils Promote Mycobacterial Trehalose Dimycolate-Induced Lung Inflammation via the Mincle Pathway. *PLoS Pathog.* 8:e1002614.

Lerm, M., and M.G. Netea. 2015. Trained immunity: a new avenue for tuberculosis vaccine development. *J. Intern. Med.*

Lin, P.L., and J.L. Flynn. 2015. CD8 T cells and Mycobacterium tuberculosis infection. *Semin. Immunopathol.* 37:239-249.

Lindsay, R.W., P.A. Darrah, K.M. Quinn, U. Wille-Reece, L.M. Mattei, A. Iwasaki, S.P. Kasturi, B. Pulendran, J.G. Gall, A.G. Spies, and R.A. Seder. 2010. CD8+ T cell responses following replication-defective adenovirus serotype 5 immunization are dependent on CD11c+ dendritic cells but show redundancy in their requirement of TLR and nucleotide-binding oligomerization domain-like receptor signaling. *J Immunol*. 185:1513-1521.

Lobato-Pascual, A., P.C. Saether, S. Fossum, E. Dissen, and M.R. Daws. 2013. Mincle, the receptor for mycobacterial cord factor, forms a functional receptor complex with MCL and FcepsilonRI-gamma. *Eur. J. Immunol.* 43:3167-3174.

Marakalala, M.J., L.M. Graham, and G.D. Brown. 2011. The role of Syk/CARD9-coupled C-type lectin receptors in immunity to Mycobacterium tuberculosis infections. *Clinical and Developmental Immunology*. 2010.

Marrakchi, H., M.-A. Lanéelle, and M. Daffé. 2014. Mycolic acids: structures, biosynthesis, and beyond. *Chem. Biol.* 21:67-85.

Matsumoto, M., T. Tanaka, T. Kaisho, H. Sanjo, N.G. Copeland, D.J. Gilbert, N.A. Jenkins, and S. Akira. 1999. A novel LPS-inducible C-type lectin is a transcriptional target of NF-IL6 in macrophages. *The Journal of immunology*. 163:5039-5048.

Miyake, Y., O.H. Masatsugu, and S. Yamasaki. 2015. C-Type Lectin Receptor MCL Facilitates Mincle Expression and Signaling through Complex Formation. *J Immunol*. 194:5366-5374.

Miyake, Y., K. Toyonaga, D. Mori, S. Kakuta, Y. Hoshino, A. Oyamada, H. Yamada, K. Ono, M. Suyama, Y. Iwakura, Y. Yoshikai, and S. Yamasaki. 2013. C-type lectin MCL is an FcRgamma-coupled receptor that mediates the adjuvanticity of mycobacterial cord factor. *Immunity*. 38:1050-1062.

Mortaz, E., I.M. Adcock, P. Tabarsi, M.R. Masjedi, D. Mansouri, A.A. Velayati, J.L. Casanova, and P.J. Barnes. 2015. Interaction of Pattern Recognition Receptors with Mycobacterium Tuberculosis. *J. Clin. Immunol.* 35:1-10.

Murray, P.R., C. Elmore, and D.J. Krogstad. 1980. The acid-fast stain: a specific and predictive test for mycobacterial disease. *Ann. Intern. Med.* 92:512-513.

Naviaux, R.K., E. Costanzi, M. Haas, and I.M. Verma. 1996. The pCL vector system: rapid production of helper-free, high-titer, recombinant retroviruses. *J. Virol.* 70:5701-5705.

Noll, H., H. Bloch, J. Asselineau, and E. Lederer. 1956. The chemical structure of the cord factor of Mycobacterium tuberculosis. *Biochim. Biophys. Acta*. 20:299-309.

Ostrop, J. 2015. Aktivierung humaner antigenpräsentierender Zellen durch den mykobakteriellen Cord-Faktor und das Glykolipid-Adjuvans Trehalose-6, 6'-dibehenate.

Ostrop, J., K. Jozefowski, S. Zimmermann, K. Hofmann, E. Strasser, B. Lepenies, and R. Lang. 2015. Contribution of MINCLE-SYK Signaling to Activation of Primary Human APCs by Mycobacterial Cord Factor and the Novel Adjuvant TDB. *J Immunol*. 195:2417-2428.

Owen, J., J. Punt, S.A. Stranford, and P.P. Jones. 2013. Kuby immunology. Freeman, New York.

Parte, A.C. 2014. LPSN--list of prokaryotic names with standing in nomenclature. *Nucleic Acids Res.* 42:D613-616 (Up to date URL: http://www.bacterio.net/mycobacterium.html).

Patin, E.C., S. Willcocks, S. Orr, T.H. Ward, R. Lang, and U.E. Schaible. 2016. Mincle-mediated anti-inflammatory IL-10 response counter-regulates IL-12 in vitro. *Innate Immun.* 22:181-185.

Petruccioli, E., A. Romagnoli, M. Corazzari, E.M. Coccia, O. Butera, G. Delogu, M. Piacentini, E. Girardi, G.M. Fimia, and D. Goletti. 2012. Specific T cells restore the autophagic flux inhibited by Mycobacterium tuberculosis in human primary macrophages. *J. Infect. Dis.* 205:1425-1435.

Pottumarthy, S., A.J. Morris, A.C. Harrison, and V.C. Wells. 1999. Evaluation of the Tuberculin Gamma Interferon Assay: Potential To Replace the Mantoux Skin Test. *J. Clin. Microbiol.* 37:3229-3232.

Poyntz, H.C., E. Stylianou, K.L. Griffiths, L. Marsay, A.M. Checkley, and H. McShane. 2014. Non-tuberculous mycobacteria have diverse effects on BCG efficacy against Mycobacterium tuberculosis. *Tuberculosis (Edinburgh, Scotland)*. 94:226-237.

Prevots, D.R., and T.K. Marras. 2015. Epidemiology of human pulmonary infection with nontuberculous mycobacteria: a review. *Clin. Chest Med.* 36:13-34.

Prevots, D.R., P.A. Shaw, D. Strickland, L.A. Jackson, M.A. Raebel, M.A. Blosky, R. Montes de Oca, Y.R. Shea, A.E. Seitz, S.M. Holland, and K.N. Olivier. 2010. Nontuberculous mycobacterial lung disease prevalence at four integrated health care delivery systems. *Am. J. Respir. Crit. Care Med.* 182:970-976.

Ryll, R., Y. Kumazawa, and I. Yano. 2001. Immunological Properties of Trehalose Dimycolate (Cord Factor) and Other Mycotic Acid-Containing Glycolipids–-A Review. *Microbiol. Immunol.* 45:801-811.

Schoenen, H., B. Bodendorfer, K. Hitchens, S. Manzanero, K. Werninghaus, F. Nimmerjahn, E.M. Agger, S. Stenger, P. Andersen, and J. Ruland. 2010. Cutting edge: Mincle is essential for recognition and adjuvanticity of the mycobacterial cord factor and its synthetic analog trehalose-dibehenate. *The Journal of Immunology*. 184:2756-2760.

Schoenen, H., A. Huber, N. Sonda, S. Zimmermann, J. Jantsch, B. Lepenies, V. Bronte, and R. Lang. 2014. Differential control of Mincle-dependent cord factor recognition and macrophage responses by the transcription factors C/EBPbeta and HIF1alpha. *J Immunol*. 193:3664-3675.

Schröder, K.-H., J. Kazda, K. Müller, and H. Müller. 1992. Isolation of Mycobacterium simiae from the environment. *Zentralblatt für Bakteriologie*. 277:561-564.

Schulze-Röbbecke, R., B. Janning, and R. Fischeder. 1992. Occurrence of mycobacteria in biofilm samples. *Tuber. Lung Dis.* 73:141-144.

Smith, D.G., and S.J. Williams. 2016. Immune sensing of microbial glycolipids and related conjugates by T cells and the pattern recognition receptors MCL and Mincle. *Carbohydr. Res.* 420:32-45.

Sridhar, S., K.S. Fung, J.F. Chan, J.Y. Lam, E.K. Yip, I.F. Hung, A.K. Wu, T.L. Que, S.K. Lau, and P.C. Woo. 2016. High recurrence rate supports need for secondary prophylaxis in non-HIV patients with disseminated mycobacterium avium complex infection: a multi-center observational study. *BMC Infect. Dis.* 16:74.

Thomson, R., C. Tolson, H. Sidjabat, F. Huygens, and M. Hargreaves. 2013. Mycobacterium abscessus isolated from municipal water-a potential source of human infection. *BMC Infect. Dis.* 13:241.

Underhill, D.M., and H.S. Goodridge. 2012. Information processing during phagocytosis. *Nat. Rev. Immunol.* 12:492-502.

van Ingen, J. 2013. Diagnosis of nontuberculous mycobacterial infections. *Semin. Respir. Crit. Care Med.* 34:103-109.

Velayati, A.A., and P. Farnia. 2012. Morphological Characterization of Mycobacterium tuberculosis. INTECH Open Access Publisher.

Venkataswamy, M.M., M.F. Goldberg, A. Baena, J. Chan, W.R. Jacobs, Jr., and S.A. Porcelli. 2012. In vitro culture medium influences the vaccine efficacy of Mycobacterium bovis BCG. *Vaccine*. 30:1038-1049.

Wagner, D., and L.S. Young. 2004. Nontuberculous mycobacterial infections: a clinical review. *Infection*. 32:257-270.

Weiss, G., and U.E. Schaible. 2015. Macrophage defense mechanisms against intracellular bacteria. *Immunol. Rev.* 264:182-203.

Wells, C.A., J.A. Salvage-Jones, X. Li, K. Hitchens, S. Butcher, R.Z. Murray, A.G. Beckhouse, Y.L. Lo, S. Manzanero, C. Cobbold, K. Schroder, B. Ma, S. Orr, L. Stewart, D. Lebus, P. Sobieszczuk, D.A. Hume, J. Stow, H. Blanchard, and R.B. Ashman. 2008. The macrophage-inducible C-type lectin, mincle, is an essential component of the innate immune response to Candida albicans. *J Immunol*. 180:7404-7413.

Wevers, B.A., T.M. Kaptein, E.M. Zijlstra-Willems, B. Theelen, T. Boekhout, T.B. Geijtenbeek, and S.I. Gringhuis. 2014. Fungal engagement of the C-type lectin mincle suppresses dectin-1-induced antifungal immunity. *Cell Host Microbe*. 15:494-505.

WHO. 2015. Global tuberculosis report 2015.

Yamasaki, S., E. Ishikawa, M. Sakuma, H. Hara, K. Ogata, and T. Saito. 2008. Mincle is an ITAM-coupled activating receptor that senses damaged cells. *Nat. Immunol.* 9:1179-1188.

Zhang, Y. 2004. Persistent and dormant tubercle bacilli and latent tuberculosis. *Front. Biosci.* 9:1136-1156.

Zhao, X.Q., L.L. Zhu, Q. Chang, C. Jiang, Y. You, T. Luo, X.M. Jia, and X. Lin. 2014. C-type lectin receptor dectin-3 mediates trehalose 6,6'-dimycolate (TDM)-induced Mincle expression through CARD9/Bcl10/MALT1-dependent nuclear factor (NF)-kappaB activation. *J Biol Chem*. 289:30052-30062.

Zhu, L.L., X.Q. Zhao, C. Jiang, Y. You, X.P. Chen, Y.Y. Jiang, X.M. Jia, and X. Lin. 2013. C-type lectin receptors Dectin-3 and Dectin-2 form a heterodimeric pattern-recognition receptor for host defense against fungal infection. *Immunity*. 39:324-334.

Zuber, B., M. Chami, C. Houssin, J. Dubochet, G. Griffiths, and M. Daffe. 2008. Direct visualization of the outer membrane of mycobacteria and corynebacteria in their native state. *J. Bacteriol.* 190:5672-5680.

References

6 Appendix

6.1 Appendix I – Settings for RT-qPCR analysis

(A)

(B)

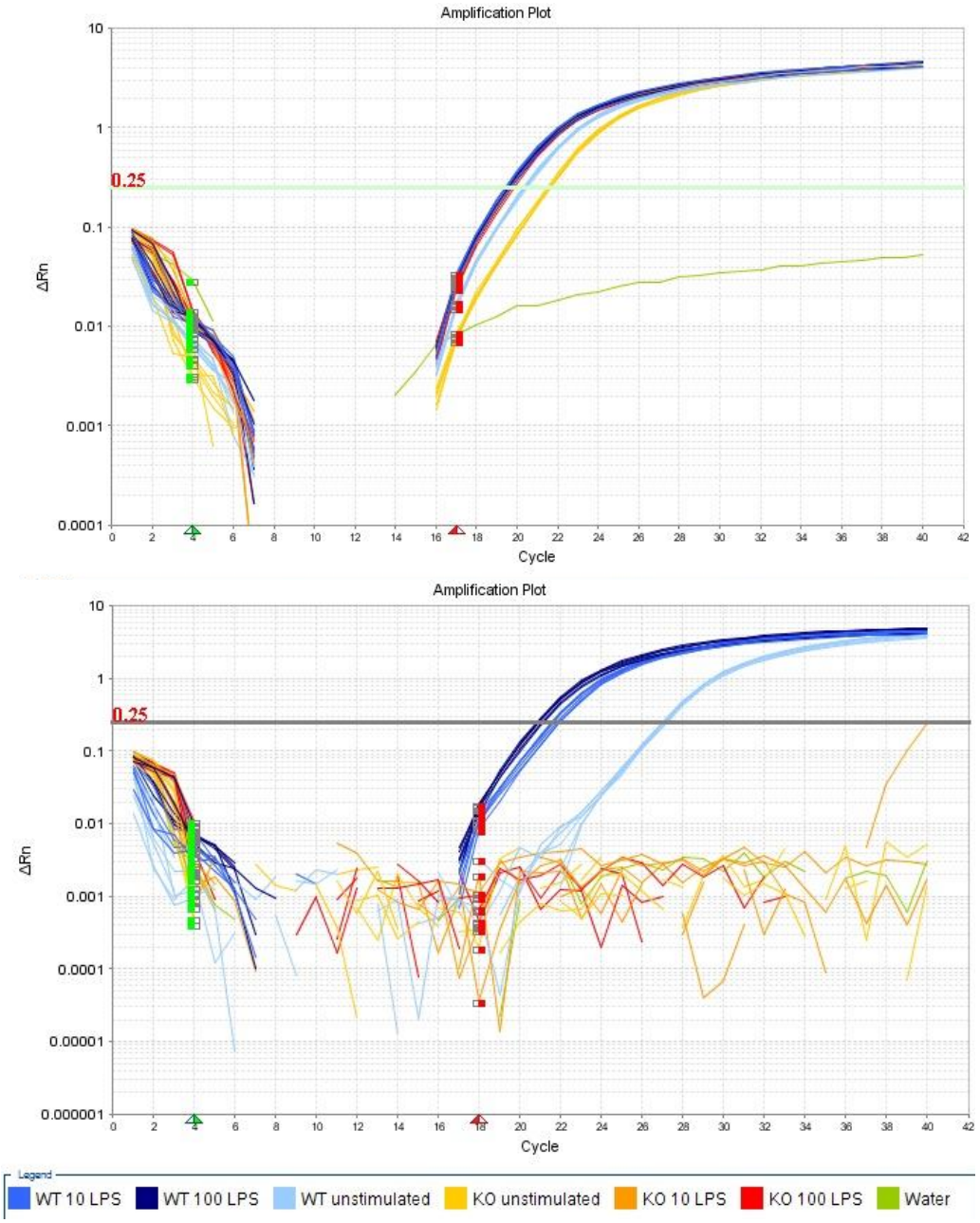

Figure 6.1 Baseline- and threshold settings for RT-qPCR analysis. The figure shows the baseline- and threshold settings used for house-keeping gene, GAPDH (A) and Mincle (B). Graphs obtained using StepOne Real-time PCR system and StepOne software (Applied Biosystems).

6.2 Appendix II – Flow gating when testing antibodies

Antibody specificity measured using transfected, over-expressing HEK293 cells in a FACSCanto II Flow cytometer.

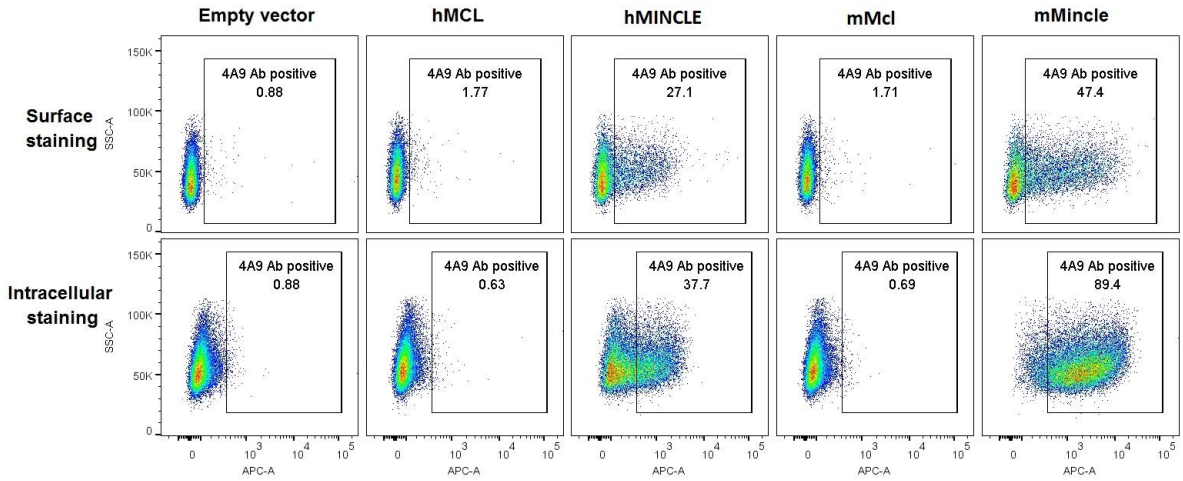

Figure 6.2 Specificity of the 4A9 Ab (α-mMincle). Pseudocolor dotplot of transfected HEK293 cells, stained with an α-mMincle Ab (4A9). Gating was done using cells transfected with an empty vector, shown to the left.

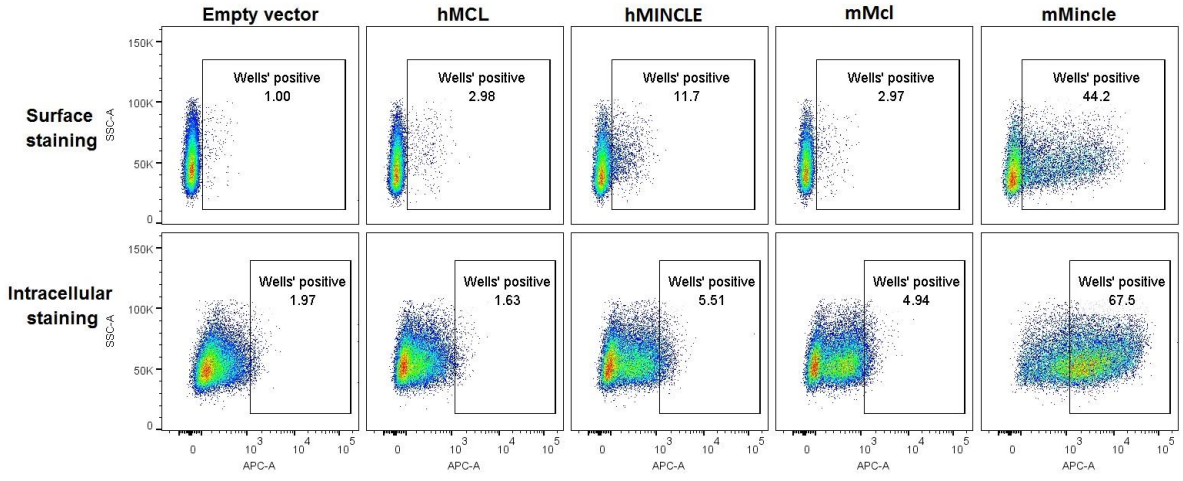

Figure 6.3 Specificity of Wells' Ab (α-mMincle). Pseudocolor dotplot of transfected HEK293 cells, stained with an α-mMincle Ab, kindly provided by Christine A. Wells. Gating was done using cells transfected with an empty vector, shown to the left.

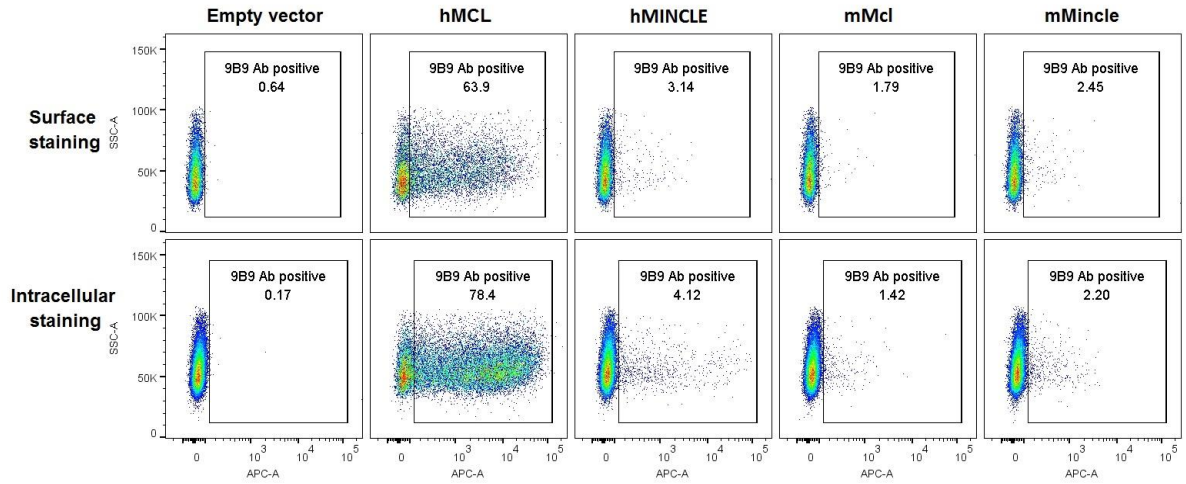

Figure 6.4 Specificity of the 9B9 Ab (α-hMcl). Pseudocolor dotplot of transfected HEK293 cells, stained with an α-hMcl Ab (9B9). Gating was done using cells transfected with an empty vector, shown to the left.

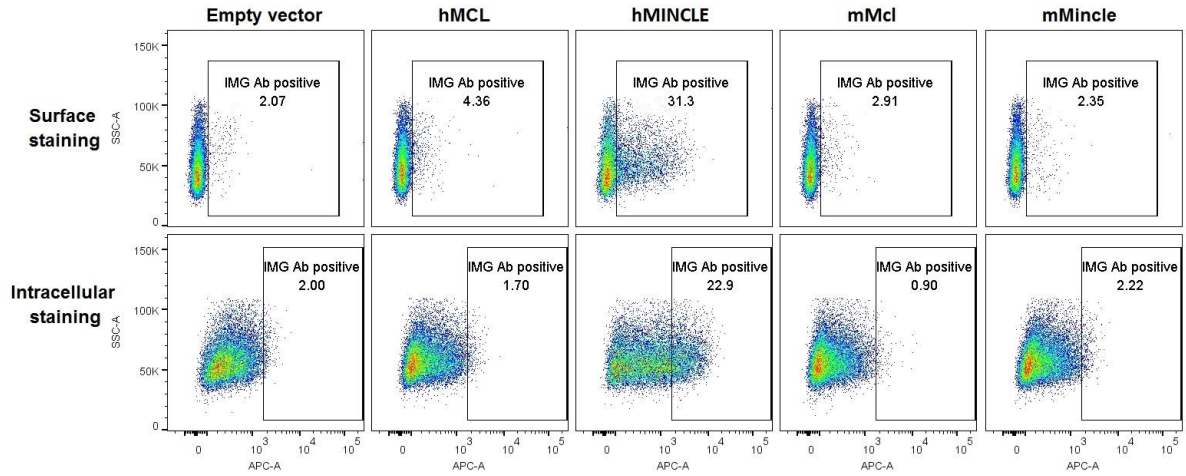

Figure 6.5 Specificity of the IMG Ab (α-hMincle). Pseudocolor dotplot of transfected HEK293 cells, stained with an α-hMincle Ab (IMG). Gating was done using cells transfected with an empty vector, shown to the left.

6.4 Appendix IV Qiagen Maxi-prep protocol

Quick-Start Protocol

EndoFree® Plasmid Maxi Kit

The EndoFree Plasmid Maxi Kit (cat. no. 12362) can be stored at room temperature (15–25°C) for up to 2 years.

For more information, please refer to the *EndoFree Plasmid Purification Handbook,* which can be found at www.qiagen.com/handbooks.

For technical assistance, please call toll-free 00800-22-44-6000, or find regional phone numbers at www.qiagen.com/contact.

Notes before starting

- Add RNase A solution to Buffer P1, mix, and store at 2–8°C.
- **Optional**: Add LyseBlue® reagent to Buffer P1 at a ratio of 1:1000.
- Prechill Buffer P3 at 4°C. Check Buffer P2 for SDS precipitation.
- Isopropanol is required.
- Add 40 ml 96—100% ethanol to the endotoxin-free water supplied with the kit.
- Use endotoxin-free or pyrogen-free plasticware (step 9 onward).

Table 1. Maximum recommended LB culture volumes

Kit	High-copy plasmid	Low-copy plasmid
EndoFree Plasmid Maxi	100 ml	250 ml

1. Harvest overnight LB culture by centrifuging at 6000 x *g* for 15 min at 4°C.
2. Completely resuspend the bacterial pellet in 10 ml Buffer P1.
3. Add 10 ml Buffer P2, mix thoroughly by inverting 4–6 times, and incubate at room temperature (15–25°C) for 5 min. If using LyseBlue reagent, the solution will turn blue.

January 2011

QIAGEN®

Sample & Assay Technologies

Quick-Start Protocol

4. During the incubation, screw the QIAfilter Cartridge cap onto the outlet nozzle of the QIAfilter Cartridge. Place the QIAfilter Cartridge in a convenient tube or in a QIArack (cat. no. 19015).
5. Add 10 ml chilled Buffer P3, mix thoroughly by inverting 4–6 times. If using LyseBlue reagent, mix the solution until it is completely colorless.
6. Pour the lysate into the barrel of the QIAfilter Cartridge. Incubate at room temperature for 10 min. Do not insert the plunger! Remove the cap from the QIAfilter Cartridge outlet nozzle. Gently insert the plunger into the QIAfilter Cartridge and filter the cell lysate into a 50 ml tube.
7. Add 2.5 ml Buffer ER to the filtered lysate, mix by inverting the tube approximately 10 times, and incubate on ice for 30 min.
8. Equilibrate a QIAGEN-tip 500 by applying 10 ml Buffer QBT, and allow the column to empty by gravity flow.
9. Apply the filtered lysate from step 7 to the QIAGEN-tip and allow it to enter the tip.
10. Wash the QIAGEN-tip with 2 x 30 ml Buffer QC.
11. Elute DNA with 15 ml Buffer QN into a 30 ml endotoxin-free or pyrogen-free tube.
12. Precipitate DNA by adding 10.5 ml (0.7 volumes) room-temperature isopropanol to the eluted DNA and mix. Centrifuge at ≥15,000 x *g* for 30 min at 4°C. Carefully decant the supernatant.
13. Wash the DNA pellet with 5 ml of endotoxin-free room-temperature 70% ethanol and centrifuge at ≥15,000 x *g* for 10 min. Carefully decant the supernatant without disturbing the pellet.
14. Air-dry the pellet for 5–10 min and redissolve the DNA in a suitable volume of endotoxin-free Buffer TE.

For up-to-date licensing information and product-specific disclaimers, see the respective QIAGEN® kit handbook or user manual.